Universitat de València
Facultat de Física

Master in Advanced Physics

Pathway in Theoretical Physics

Final Master's Thesis

A SCALAR EXTENSION OF THE SM. THE HIGGS TRIPLET MODEL

Javier Castellano Ruiz

Supervisor: Antonio Pich Zardoya

Academic year: 2016-2017

Abstract

In 2012, the ATLAS and CMS experiments at LHC announced the discovery of a new scalar particle with a mass around 126 GeV consistent with the Higgs boson predicted by the Standard Model. The discovery of this particle and the measurement of its properties has been seen as a final test for the Standard Model to be considered the theory of physics at this energy region. Nevertheless, it is clear that there should be some new physics appearing at higher energies. Some extensions of the SM consider models for which this new physics appears around the TeV scale, allowing those models to be tested at the LHC. The Higgs sector presents an opportunity for looking for physics beyond the Standard Model because of its yet to be fully determined nature, allowing for a wide variety of modifications. Here, an extension of the scalar sector by introducing a triplet with hypercharge $y_\delta = 2$ is proposed and the consequences and possible tests have been studied.

Contents

1 Introduction

The Standard Model is - until now - the best recipe of how three of the fundamental forces and particles are related, and provides a description of all - so far known - elementary particles. Developed in the early 1970s, it has successfully explained wide variety of phenomena and has been able to predict with an outstanding agreement a large number of experimental results. Even though the SM is currently the best description, it is certainly known that it is not the theory that will explain the complete picture, from the neutrinos masses up to the Planck scale.

Within the SM, a scalar doublet is introduced and the symmetry gets spontaneously broken when the neutral field acquires a vacuum expectation value. Then, three degrees of freedom are rotated becoming the longitudinal polarizations of the $W^{\pm}$ and Z gauge bosons, allowing them to have mass. From the four initial degrees of freedom introduced by the doublet, after the SSB and the field rotation, there is a remaining neutral scalar particle that couples with all massive SM particles. Therefore, this so-called Higgs boson is a testable manifestation of the Brout-Englert-Higgs mechanism. This mechanism has been considered tested as in 2012, the ATLAS and CMS collaborations from the LHC announced they observed a new particle in the mass region around 126 GeV consistent with the Higgs boson arising from this SSB mechanism [1–4]. Another possibility still considered is that this scalar particle is not the Higgs boson predicted by the Standard Model, but those theories are expected become more constrained as the LHC collects more data.

Although the Standard Model accurately describes phenomena within this energy region, there are strong evidences supporting the idea that the SM could be contained inside a more general one. The community expects that new data from experiments at the LHC could lead to these missing pieces, setting the path to establishing a new theory beyond the Standard Model (BSM). There are two main approaches considered for studying physics BSM. The first would be considering a whole new theory that contains the SM as an effective theory at low energies, that is the case for Supersymmetric Models (SSM) or String theory. The second one would be to consider extensions to the SM. In this case, these extensions propose solutions to some phenomena which explanation is not contained in the SM. This second approach is what led to the introduction of models such as the seesaw mechanisms.

In the SM, neutrinos are massless and strictly left-chiral particles. With neutrino oscillations definitively observed, it is known experimentally that neutrinos have non-zero masses. Therefore, one attractive extension that allows for non-zero masses and also predicts them to be light is the so called see-saw mechanism.

Here, a scalar extension of the SM by introducing a scalar triplet with hypercharge $y_\delta = 2$ is presented. This extension of the scalar sector was first introduced within the scenario of generating neutrino masses, via the so-called type II seesaw mechanism [5, 6]. The model introduces, after the SSB and alongside with the 3 Goldstone bosons to be "eaten" by the gauge bosons, two CP-even scalars (h, H), a CP-odd scalar (θ), a charged and a doubly-charged scalars ($H^\pm$, $\delta^{\pm\pm}$). We will consider the lightess of the CP-even scalars to be the scalar particle discovered at the LHC. Even if within this model the Higgs boson is a mixture of a doublet and a triplet scalars, the constraints on the mixture will require for a SM-like behaviour. As the model introduces new particles coupling to the SM ones, the radiative corrections to the electroweak parameters have been considered [7]. The one-loop contributions to the W boson mass as well as to the ρ parameter are key for setting constraints in the mass spectrum of the new particles. In Section 3.3, the decay rate of the Higgs boson into two photons is evaluated as this decay channel could present measurable discrepancies from the SM.

1.1 Scalar extensions of the SM

Even though the Higgs mechanism was first introduced by adding a scalar doublet to the SM, there is not any theoretical or phenomenological restriction for the scalar sector to be fixed on a single scalar doublet. In fact, the Higgs mechanism could be accomplished as well by higher representations of $SU(2)_L$. Consequently, extensions of the Standard Model in which the scalar content is enlarged have been regularly considered.

An extended scalar sector with several fields belonging to different $SU(2)_L \otimes U(1)_Y$ representations (T_i, y_i)[1] would lead in general to a different relation between the gauge-boson masses. At tree level, the following result can be easily derived:

$$\rho \equiv \frac{m_W^2}{m_Z^2 \cos^2\theta_W} = \frac{\sum\limits_i v_i^2 \left[T_i(T_i+1) - \left(\frac{y_i}{2}\right)^2 \right]}{2 \sum\limits_i v_i^2 \left(\frac{y_i}{2}\right)^2}, \tag{1.1}$$

where $v_i/\sqrt{2}$ is the vacuum expectation value of the neutral field component of the multiplet. From (1.1), it can be seen that extensions of the scalar sector by adding singlets ($y_i = T_i = 0$) [8, 9] and doublets ($y_i = 1$, $T_i = 1/2$) [10–12] of $SU(2)_L$ have been frecuently considered as they maintain the SM prediction of $\rho = 1$ at tree level without imposing restrictions on the vacuum expectation values or requiring from fine-tunning.

Scalar multiplets of higher $SU(2)_L$ representations would imply a different prediction of the ρ parameter, unless their hypercharges are conveniently tuned. This fact would result in doublets and singlets to be the prefered candidates for building extensions of the SM. Nevertheless, the introduction of a triplet scalar of hypercharge $y_\delta = 2$ became interesting because of the type-II seesaw mechanism [5,6], as will be discussed later in Section 2.4.

[1] In this work, the definition of hypercharge $y = 2(Q - T_3)$ will be used.

2 The Higgs triplet model

In this Chapter the introduction of the Higgs triplet model[1] will be performed. The procedure will be conceptually equivalent as done for the doublet in the SM [13]. In Section 2.1, the covariant derivative for the triplet and the most general scalar potential for the scalar sector will be defined. The gauge boson masses will appear after the symmetry gets spontaneously broken and the doublet and triplet neutral components acquire a vacuum expectation value (vev). Now the gauge boson masses will depend not only on the vev acquired by the doublet, but on a combination of both vev. The masses of the scalar particles will be computed and expressed in terms of the parameters of the scalar potencial, this will be done in Section 2.2. Theoretical constraints coming from unitarity, vacuum stability and the absence of tachyonic modes will be discussed in Section 2.3. Finally, the seesaw type II will be briefly explained in Section 2.4 as well as some implications for the leptonic sector will be summarised in Section 2.5.

2.1 The Scalar potential in the doublet-triplet Higgs model

Within the Higgs triplet model (HTM) the scalar sector consists of the standard Higgs weak doublet Φ and a colorless scalar triplet Δ with hypercharge $y_\delta = 2$ and transforming as $(1,3,2)$ under $SU(3)_C \otimes SU(2)_L \otimes U(1)_Y$. Under a general gauge transformation $\mathcal{U}(x)$, Φ and Δ transform as $\Phi \to \mathcal{U}(x)\Phi$ and $\Delta \to \mathcal{U}(x)\,\Delta\,\mathcal{U}^\dagger(x)$. One could then write the most general renormalizable and gauge invariant Lagrangian for this scalar sector:

$$\mathcal{L} \;=\; (D_\mu\Phi)^\dagger(D^\mu\Phi) + \mathrm{Tr}\big[(D_\mu\Delta)^\dagger(D^\mu\Delta)\big] - V(\Phi,\Delta) + \mathcal{L}_{\mathrm{Y}}, \tag{2.1}$$

where the covariant derivatives are defined by

$$D_\mu\Phi = \partial_\mu\Phi + igT^aW^a_\mu\Phi + i\frac{g'}{2}B_\mu\Phi, \tag{2.2}$$

$$D_\mu\Delta = \partial_\mu\Delta + ig[T^aW^a_\mu,\Delta] + ig'\frac{y_\delta}{2}B_\mu\Delta, \tag{2.3}$$

denoting respectively the $SU(2)_L$ and $U(1)_Y$ gauge fields and couplings by (W^a_μ, g) and (B_μ, g').

[1] Sometimes refered as well as doublet-triplet Higgs model (DTHM).

$T^a \equiv \sigma^a/2$ are the generators of the $SU(2)_L$ transformations, with σ^a ($a = 1, 2, 3$) the Pauli matrices.

The most general potential for the HTM, $V(\Phi, \Delta)$, including all possible gauge invariant and renormalizable operators can be defined as:

$$\begin{aligned} V(\Phi, \Delta) &= -m_\Phi^2 \Phi^\dagger \Phi + M^2 \,\mathrm{Tr}(\Delta^\dagger \Delta) + \left[\mu(\Phi^T i\sigma^2 \Delta^\dagger \Phi) + \mathrm{h.c.}\right] + \frac{\lambda}{4}(\Phi^\dagger \Phi)^2 \\ &\quad + \lambda_1 (\Phi^\dagger \Phi) \,\mathrm{Tr}(\Delta^\dagger \Delta) + \lambda_2 \left[\mathrm{Tr}(\Delta^\dagger \Delta)\right]^2 + \lambda_3 \,\mathrm{Tr}\left[(\Delta^\dagger \Delta)^2\right] + \lambda_4 \Phi^\dagger \Delta \Delta^\dagger \Phi, \end{aligned} \tag{2.4}$$

where all the parameters can be taken to be real without any loss of generality [14, 15]. As the quartic field terms must be self-Hermitian, the parameters λ, λ_1 to λ_4 should be real. For the cubic term, even if μ is introduced as a complex parameter, its phase could be absorbed by a redefinition of the Φ and Δ fields, meaning that the potential does not include any source of CP violation [15]. For the m_Φ^2 and M^2 parameters, it will be explicit later in Equations (2.10) and (2.11) that they could be traded for μ, λ_i and the vev, that could be aligned without any loss of generality, therefore resulting to be real. A term of the form $\lambda_5 \Phi^\dagger \Delta^\dagger \Delta \Phi$ could be absorbed into the λ_1 and λ_4 terms appearing in Eq. (2.4) thanks to the identity $\Phi^\dagger \Delta^\dagger \Delta \Phi + \Phi^\dagger \Delta \Delta^\dagger \Phi = \Phi^\dagger \Phi \,\mathrm{Tr}(\Delta^\dagger \Delta)$.

The cubic term parameter μ introduces an explicit violation of the lepton number at the Lagrangian level once Δ is assigned to carry a non-zero lepton number, $L = 2$. Some studies were performed where a $U(1)_{\mathrm{Lep}}$ symmetry was imposed and μ was constrained to be zero [16, 17]. The requirement on μ to be zero introduces a massless neutral physical pseudoscalar, θ, the would-be Majoron, a Goldstone boson appearing from the fact that the initially preserved symmetry of lepton number gets spontaneously broken once the triplet acquires a vacuum expectation value. However, these models were discarded as they predict an increase on the invisible decay width of the Z boson. One should note that this model contains two sources of lepton number violation, μ and the coupling of the triplet particles with the $SU(2)_L$ lepton doublets. If one requires the lepton number not to be strongly violated only small values for μ should be considered, although all possibilities will be explored here.

Note that in the bilinear term in (2.4), a "wrong sign" is used for the mass term of the doublet fields while the "correct sign" appears for mass of the triplet fields. This configuration is required in the case of the doublet fields for spontaneous symmetry breaking to take place and, regarding the triplet fields, for keeping the triplet vev naturally small without the appearance of tachyonic modes or involving fine-tunning.

The $\mathcal{L}_{\mathrm{Y}}$ term in (2.1) contains all the Yukawa sector, being that of the SM plus the extra Yukawas coupling the $SU(2)_L$ doublets with the Higgs triplet. The new Yukawa leads to a Majorana mass terms for neutrinos once the neutral component of Δ acquires a vacuum expectation value (vev). This will be discussed in more detail in Section 2.4.

The two Higgs multiplets can be defined in components as follows:

$$\Delta = \begin{pmatrix} \delta^+/\sqrt{2} & \delta^{++} \\ \delta^0 & -\delta^+/\sqrt{2} \end{pmatrix} \quad \text{and} \quad \Phi = \begin{pmatrix} \phi^+ \\ \phi^0 \end{pmatrix}, \tag{2.5}$$

that can be redefined after spontaneous symmetry breaking as

$$\Delta \;= \frac{1}{\sqrt{2}} \begin{pmatrix} \omega_\delta^+ & \sqrt{2}\,\delta^{++} \\ v_\delta + h_\delta + i\eta_\delta & -\omega_\delta^+ \end{pmatrix} \quad \text{and} \quad \Phi = \frac{1}{\sqrt{2}} \begin{pmatrix} \sqrt{2}\,\omega_\phi^+ \\ v_\phi + h_\phi + i\eta_\phi \end{pmatrix}, \tag{2.6}$$

in such a way that they do not get any vev: $\phi \to \phi + \langle\phi\rangle$. In both cases a 2×2 traceless matrix representation of the triplet has been used.

As stated before, one of the strong constraints on the Higgs triplet model comes from the extremely well measured ρ parameter ($\rho \equiv m_W/m_Z \cos\theta_W$) as the electroweak precision data constraints require not to deviate notably from the value predicted within the SM. At tree level the SM model prediction is $\rho_{\text{SM}}^{\text{tree}} = 1$, and from the global fit $\rho_{\text{exp}} = 1.00037 \pm 0.00023$ [18]. From Equation (1.1), at tree level for the HTM:

$$\rho = \frac{v_\phi^2 + 2v_\delta^2}{v_\phi^2 + 4v_\delta^2}, \tag{2.7}$$

and the gauge boson masses are now:

$$m_Z^2 = \frac{g^2}{4\,c_W^2}\left(v_\phi^2 + 4v_\delta^2\right), \qquad m_W^2 = \frac{g^2}{4}\left(v_\phi^2 + 2v_\delta^2\right). \tag{2.8}$$

The ρ parameter could be approximated as:

$$\rho = \frac{v_\phi^2 + 2v_\delta^2}{v_\phi^2 + 4v_\delta^2} \simeq 1 - 2\alpha^2, \tag{2.9}$$

where the parameter $\alpha \equiv v_\delta/v_\phi$ has been defined. Identifying $\delta\rho \equiv \rho - \rho_{\text{SM}} = -2\alpha^2$, this result requires for a small value of v_δ compared to the electroweak scale in order to keep the value of the ρ parameter close to the SM prediction. This condition just set on v_δ allows for a small value for the neutrino masses without the need of fine-tunning.

2.2 The field composition of the model

Once the potencial has been introduced a study on the field composition of the model can be performed. From Eq. (2.4) and requiring the potential to be localized at a minimum the number of parameters of the model can be reduced by a number of two, as:

$$m_\Phi^2 \;=\; \frac{\lambda v_\phi^2}{4} + \frac{(\lambda_1 + \lambda_4)v_\delta^2}{2} - \sqrt{2}\mu v_\delta\,, \tag{2.10}$$

$$M^2 \;=\; -(\lambda_2 + \lambda_3)v_\delta^2 - \frac{(\lambda_1 + \lambda_4)v_\phi^2}{2} + \frac{\mu v_\phi^2}{\sqrt{2}v_\delta}\,. \tag{2.11}$$

Computing the mass matrices from Eq. (2.4), the following result is obtained:

$$\mathcal{M}^2 = \begin{pmatrix} m^2_{\delta^{\pm\pm}} & & & \\ & \boxed{\mathcal{M}^2_{\pm}} & & \\ & & \boxed{\mathcal{M}^2_{\rm odd}} & \\ & & & \boxed{\mathcal{M}^2_{\rm even}} \end{pmatrix}, \tag{2.12}$$

i.e., the mass matrix can be decomposed into three 2×2 mass matrices and the mass squared of the doubly-charged field. These matrices get the form:

$$\mathcal{M}^2_{\pm} = \begin{pmatrix} -\frac{\lambda_4}{2} v_\delta^2 + \sqrt{2}\mu v_\delta & -\mu v_\phi + \frac{\lambda v_\phi^2}{2\sqrt{2}} \\ -\mu v_\phi + \frac{\lambda v_\phi^2}{2\sqrt{2}} & -\frac{\lambda_4}{4} v_\phi^2 + \frac{\mu\, v_\phi^2}{\sqrt{2} v_\delta} \end{pmatrix}, \qquad \mathcal{M}^2_{\rm even} = \begin{pmatrix} A_H & -B_H \\ -B_H & C_H \end{pmatrix}, \tag{2.13}$$

$$\mathcal{M}^2_{\rm odd} = \begin{pmatrix} 2\sqrt{2}\mu v_\delta & -\sqrt{2}\mu v_\phi \\ -\sqrt{2}\mu v_\phi & \frac{\mu\, v_\phi^2}{\sqrt{2} v_\delta} \end{pmatrix}, \tag{2.14}$$

being A_H, B_H and C_H:

$$A_H = \frac{\lambda}{2} v_\phi^2, \tag{2.15}$$

$$B_H = \sqrt{2}\mu v_\phi - (\lambda_1 + \lambda_4) v_\delta v_\phi, \tag{2.16}$$

$$C_H = \frac{\mu}{\sqrt{2}} \frac{v_\phi^2}{v_\delta} + 2(\lambda_2 + \lambda_3) v_\delta^2. \tag{2.17}$$

The fields in Eq. (2.6) can then be rotated into the physical fields as follows:

$$\begin{pmatrix} h \\ H \end{pmatrix} = \begin{pmatrix} c_\alpha & s_\alpha \\ -s_\alpha & c_\alpha \end{pmatrix} \begin{pmatrix} h_\phi \\ h_\delta \end{pmatrix}, \qquad \begin{pmatrix} \zeta \\ \theta \end{pmatrix} = \begin{pmatrix} c_\tau & s_\tau \\ -s_\tau & c_\tau \end{pmatrix} \begin{pmatrix} \eta_\phi \\ \eta_\delta \end{pmatrix}, \tag{2.18}$$

$$\begin{pmatrix} \omega^\pm \\ H^\pm \end{pmatrix} = \begin{pmatrix} c_\beta & s_\beta \\ -s_\beta & c_\beta \end{pmatrix} \begin{pmatrix} \omega_\phi^\pm \\ \omega_\delta^\pm \end{pmatrix}. \tag{2.19}$$

Here, h and H correspond to the CP-even neutral scalars, while θ is CP-odd. ζ and $\omega^\pm$ are the would-be Goldstone bosons associated to the Z and $W^\pm$ gauge bosons respectively (see Appendix B). Finally, $H^\pm$ and $\delta^{\pm\pm}$ are the charged and doubly charged scalars.

The triplet-doublet mixing angles are defined as:

$$\tan 2\alpha = \frac{2B_H}{C_H - A_H} = \frac{\left(\sqrt{2}\mu - (\lambda_1 + \lambda_4)v_\delta\right)v_\phi}{\left(\frac{\mu}{2\sqrt{2}v_\delta} - \frac{\lambda}{4}\right)v_\phi^2 + (\lambda_2 + \lambda_3)v_\delta^2}, \tag{2.20}$$

$$\tan\beta = \frac{\sqrt{2}v_\delta}{v_\phi}, \tag{2.21}$$

$$\tan\tau = \frac{2v_\delta}{v_\phi}, \tag{2.22}$$

and the masses of the physical fields are the following:

(i) Doubly charged scalar:

$$m_{\delta^{++}}^2 = \frac{\mu v_\phi^2}{\sqrt{2}v_\delta} - \frac{\lambda_4}{2}v_\phi^2 - \lambda_3 v_\delta^2 \,. \tag{2.23}$$

(ii) Charged scalars:

$$m_{H^+}^2 = \frac{(2\sqrt{2}\mu - \lambda_4 v_\delta)}{4v_\delta}(v_\phi^2 + 2v_\delta^2)\,, \tag{2.24}$$

$$m_{\omega^+}^2 = 0. \tag{2.25}$$

(iii) CP-odd scalars:

$$m_\theta^2 = \frac{\mu}{\sqrt{2}v_\delta}(v_\phi^2 + 4v_\delta^2)\,, \tag{2.26}$$

$$m_\zeta^2 = 0. \tag{2.27}$$

(iv) CP-even scalars:

$$m_h^2 = \frac{1}{2}\left(A_H + C_H - \sqrt{(A_H - C_H)^2 + 4B_H^2}\right)\,, \tag{2.28}$$

$$m_H^2 = \frac{1}{2}\left(A_H + C_H + \sqrt{(A_H - C_H)^2 + 4B_H^2}\right)\,, \tag{2.29}$$

which have been defined in terms of the potential parameters from (2.4). For the CP-even part, the expressions for masses are more complex and have been defined in terms of A_H, B_H and C_H from Equations (2.15-2.17).

From Equations (2.11) and (2.23-2.24), it can be derived that in the $m_{\delta^{++}}, m_{H^+} \gg v$ limit, i.e. $m_{\delta^{++}} \sim m_{H^+} \sim$ TeV, an approximate relation for the triplet vev can be derived:

$$v_\delta \approx \frac{\mu v_\phi^2}{\sqrt{2}M^2}, \tag{2.30}$$

where M stands either for $m_{\delta^{++}}$ or m_{H^+}. From this relation, a simplified expression for $\tan 2\alpha$ and $\sin\alpha$ is obtained:

$$\tan 2\alpha \simeq \frac{4v_\delta}{v_\phi}, \qquad \sin\alpha \simeq \frac{2v_\delta}{v_\phi}. \tag{2.31}$$

Therefore, the dimensionless quantity μ/v_δ could be accepted to be larger than any other quartic coupling (λ_i) in the model, as those couplings are expected to be at most of order 10 because of unitarity. This will be discussed later in Section 3.1.

Thus, $A_H,\ C_H >> B_H$, and the masses of the h and H scalars simplify to:

$$m_h^2 \approx \frac{1}{2}\left(A_H + C_H - |A_H - C_H|\right) = \frac{\lambda}{2} v_\phi^2\,, \tag{2.32}$$

$$m_H^2 \approx \frac{1}{2}\left(A_H + C_H + |A_H - C_H|\right) = \frac{\mu}{\sqrt{2} v_\delta} v_\phi^2\,. \tag{2.33}$$

It is found that, in addition to the three Goldstone bosons ($\omega^\pm,\ \zeta$) that get absorbed as the longitudinal degree of freedom of the $W^\pm$ and Z gauge bosons, there remain seven physical fields: $\delta^{\pm\pm}$, $H^\pm$, θ, H and h. If the field h is accepted to be the Higgs boson discovered at the LHC [2], then $\mu/v_\delta > \lambda/\sqrt{2}$ as stated before. From the electroweak precision data for the ρ parameter the constraint that the mixing between the triplet and doublet Higgs multiplets should be very small, i.e. $v_\delta/v_\phi \ll 1$ is obtained, and therefore the triplet-doublet mixing angles can simplify to:

$$s_\alpha \approx 2v_\delta/v_\phi, \qquad c_{\alpha,\tau,\beta} \approx 1, \tag{2.34}$$

$$s_\tau \approx 2v_\delta/v_\phi, \tag{2.35}$$

$$s_\beta \approx \sqrt{2} v_\delta/v_\phi, \tag{2.36}$$

which requires h to behave as the SM Higgs boson up to a v_δ/v_ϕ correction, while the remaining particles correspond mostly to the components of the triplet. By looking at the expression for the masses from Eqs. (2.23-2.29), an interesting relation between the masses of the triplet-like fields arises if the parameters of the potential are supposed to be of the same order:

$$m_{\delta^{++}}^2 - m_{H^+}^2 = m_{H^+}^2 - m_\theta^2 = -\frac{\lambda_4}{4} v_\phi^2 + \mathcal{O}(v_\delta^2) \simeq -\frac{\lambda_4}{4} v_\phi^2. \tag{2.37}$$

This was done in the literature [7], where the parameter Δm is defined as:

$$\Delta m \equiv m_{\delta^{++}} - m_{H^+}. \tag{2.38}$$

In this approximation there are two configurations allowed in addition to the degenerated case, $m_{\delta^{++}} \approx m_{H^+} \approx m_\theta$, depending on the sign of the λ_4 parameter, being $m_{\delta^{++}} > m_{H^+} > m_\theta$ ($m_\theta > m_{H^+} > m_{\delta^{++}}$) for $\lambda_4 < 0$ ($\lambda_4 > 0$). The degeneracy on masses of the $\delta^{\pm\pm}$, $H^\pm$ and θ states would depend on the relation between μ/v_δ and λ_4. This behaviour will be studied later in Section 3.1.

2.3 Theoretical constraints on the potential

The model has been introduced and the fields have been defined in terms of the parameters of the potential. Before immersing into phenomenology, a previous study should be performed from theoretical constraints. Even if the parameters introduced by the scalar potential could be determined from its appearance in the couplings of the triplet and doublet fields, some strong constraints on those parameters can be derived using arguments such as unitarity and vacuum stability.

[2]The other possibility, H being lighter than h, is still allowed by the data.

Vacuum stability

A necessary condition for the stability of the vacuum is for the potential to be bounded from below when the scalar fields become large, i.e. there should not be any direction in the field space along in which the potential becomes infinitely negative. This requirement should be realised in any direction of the field space. The constraints ensuring boundedness from below (BFB) read [19]:

$$\begin{aligned}&\left\{\lambda \geq 0\,,\ \ \lambda_2+\lambda_3 \geq 0\,,\ \ \lambda_2+\frac{\lambda_3}{2} \geq 0\,,\ \ \lambda_1+\sqrt{\lambda(\lambda_2+\lambda_3)} \geq 0\,,\ \ \lambda_1+\lambda_4+\sqrt{\lambda(\lambda_2+\lambda_3)} \geq 0\right\}\\ &\quad\wedge\left\{|\lambda_4|\sqrt{\lambda_2+\lambda_3}-\lambda_3\sqrt{\lambda} \geq 0\,,\ \ \vee\ 2\lambda_1+\lambda_4+\sqrt{\left(2\lambda\lambda_3-\lambda_4^2\right)\left(\frac{2\lambda_2}{\lambda_3}+1\right)} \geq 0\right\}\,,\end{aligned} \tag{2.39}$$

where $\wedge$ ($\vee$) stand for AND (OR). These conditions have been obtained in [19], where a parametrization method has been used. The procedure will be summarised here.

In the most general scalar potential for this model, even if there are ten degrees of freedom, the potential is expressed in terms of only four quantities: $\Phi^\dagger\Phi$, Tr $\left(\Delta^\dagger\Delta\right)$, $\Phi^\dagger\Delta\Delta^\dagger\Phi$ and Tr $\left(\Delta^\dagger\Delta\Delta^\dagger\Delta\right)$. From this and accepting the quantity Tr $\left(\Delta^\dagger\Delta\right)$ to be non zero, the dimensionless parameters r, ζ and ξ can be defined as:

$$\Phi^\dagger\Phi = r\,\mathrm{Tr}\left(\Delta^\dagger\Delta\right)\,, \tag{2.40}$$

$$\mathrm{Tr}\left(\Delta^\dagger\Delta\right)^2 = \zeta\left[\mathrm{Tr}\left(\Delta^\dagger\Delta\right)\right]^2\,, \tag{2.41}$$

$$\Phi^\dagger\Delta\Delta^\dagger\Phi = \xi\,\mathrm{Tr}\left(\Delta^\dagger\Delta\right)\left(\Phi^\dagger\Phi\right)\,, \tag{2.42}$$

these parameters are defined to be $r \in (0,\infty)$, $\xi \in [0,1]$ and $\zeta \in [1/2,1]$, as stated in [19, 20]. From this definitions, the quartic terms from the potential can be rewritten in a more suitable $V^{(4)}(x) = ax^4+bx^2+c$ form:

$$\frac{V^{(4)}}{\left[\mathrm{Tr}\left(\Delta^\dagger\Delta\right)\right]^2} = \frac{\lambda}{4}r^2+(\lambda_1+\xi\lambda_4)\,r+(\lambda_2+\zeta\lambda_3)\,, \tag{2.43}$$

for which the BFB conditions are immediate:

$$a \geq 0, \qquad c \geq 0, \qquad b+2\sqrt{ac} \geq 0. \tag{2.44}$$

For the scalar potential of the HTM, those expressions become:

$$0 \leq \lambda, \tag{2.45}$$

$$0 \leq \lambda_2+\zeta\lambda_3 \equiv f_1(\zeta), \tag{2.46}$$

$$0 \leq (\lambda_1+\xi\lambda_4)+2\sqrt{\lambda(\lambda_2+\zeta\lambda_3)} \equiv f_2(\zeta,\xi), \tag{2.47}$$

that should be satisfied for all values of ξ and ζ. These conditions have been used in [19] to reach the final result shown in Equation (2.39). Nevertheless, it should be known that these conditions are sufficient, but not necessary, i.e. all potentials that satisfy these conditions will be bounded from below, although not all the potentials that are bounded from below should satisfy these conditions.

Unitarity

Some other constraints on the scalar potential parameters can be obtained by demanding tree-level unitarity for the S-matrix. This study should be performed for any possible scattering process coming from the potential. Here, the results from [20] for the HTM are summarized, where the conditions that follow have been derived only from 2-body scalar scattering processes dominated by quartic interactions:

$$\left|\lambda + 4\lambda_2 + 8\lambda_3 \pm \sqrt{(\lambda - 4\lambda_2 - 8\lambda_3)^2 + 16\lambda_4^2}\right| \leq 64\pi\,, \tag{2.48.1}$$

$$\left|3\lambda + 16\lambda_2 + 12\lambda_3 \pm \sqrt{(3\lambda - 16\lambda_2 - 12\lambda_3)^2 + 24(2\lambda_1 + \lambda_4)^2}\right| \leq 64\pi\,, \tag{2.48.2}$$

$$|\lambda| \leq 32\pi\,, \tag{2.48.3}$$

$$|2\lambda_1 + 3\lambda_4| \leq 32\pi\,, \tag{2.48.4}$$

$$|2\lambda_1 - \lambda_4| \leq 32\pi\,, \tag{2.48.5}$$

$$|\lambda_1| \leq 16\pi\,, \tag{2.48.6}$$

$$|\lambda_1 + \lambda_4| \leq 16\pi\,, \tag{2.48.7}$$

$$|2\lambda_2 - \lambda_3| \leq 16\pi\,, \tag{2.48.8}$$

$$|\lambda_2| \leq 8\pi\,, \tag{2.48.9}$$

$$|\lambda_2 + \lambda_3| \leq 8\pi\,. \tag{2.48.10}$$

The reason why only the scattering processes coming from the quartic terms of the potential have been considered is that the study of unitarity has been performed in the large $\sqrt{s}$ limit, i.e. in the limit where the energies of the processes are larger than any other mass scale in the theory. Therefore, all the parameters with a non zero mass dimension have been neglected in comparison to $\sqrt{s}$.

The unitarity condition for the T-matrices to be satisfied can be expressed as follows:

$$-\,i(T - T^\dagger) \sim \int dX_{\text{LIPS}}\, TT^\dagger. \tag{2.50}$$

Although the unitarity constraints could be obtained directly from (2.50), a more efficient study could be achieved when working with a diagonal matrix and its eigenvalues. Thus, the usual unitarity bound on partial-wave amplitudes that is valid for elastic scattering would apply directly to all the eigenvalues, obtaining the bounds on all the components of the T-matrix. In [20], a modified diagonal matrix have been defined and the conditions (2.48.1-2.48.10) were obtained.

Absence of tachyonic modes

Constrains on μ can be derived by demanding the positivity of the masses of the different fields. The positivity of m_h^2 fixes μ to lie in the range $\mu_- \leq \mu \leq \mu_+$, where:

$$\mu_\pm = \frac{\lambda v_\phi^2 + 8(\lambda_1 + \lambda_4)v_\delta^2 \pm \sqrt{\lambda(\lambda v_\phi^4 + 16 v_\delta^2((\lambda_1 + \lambda_4)v_\phi^2 + 4(\lambda_2 + \lambda_3)v_\delta^2))}}{8\sqrt{2}v_\delta}. \tag{2.51}$$

Note that $\mu_\pm$ should always be real-valued otherwise h could be tachyonic for all values of μ. This requirement leads in principle to an extra constraint, being [20]

$$\lambda\Big[\lambda v_\phi^4 + 16\, v_\delta^2\Big((\lambda_1 + \lambda_4)v_\phi^2 + 4(\lambda_2 + \lambda_3)v_\delta^2\Big)\Big] \geq 0. \tag{2.52}$$

However, this extra constraint is automatically satisfied due to the BFB constraints.

Requiring the absence of tachyonic modes for the CP-odd scalar and the singly-charged and doubly-charged scalars another three requirements are obtained:

$$\mu > 0, \tag{2.53}$$
$$\mu > \frac{\lambda_4 v_\delta}{2\sqrt{2}}, \tag{2.54}$$
$$\mu > \frac{\lambda_4 v_\delta}{\sqrt{2}} + \sqrt{2}\frac{\lambda_3 v_\delta^3}{v_\phi^2}. \tag{2.55}$$

The set of inequalities obtained using the different arguments will impose strong constraints on the possible scalar masses. This will be explored more in detail in Section 3.1.

2.4 Motivations for the HTM: The type-II seesaw mechanism

Neutrinos, as well as the scalar sector, are appealing particles for the study of new physics BSM as they are the only known fermions which are neutral with respect to all conserved charges, namely electric charge and colour. As a result, they can be Majorana particles, which leads to the question of whether they have Majorana or Dirac masses. Although a minimal extension of the SM by adding three right-handed neutrinos leading to Dirac mass terms is still allowed by phenomenology, this receipt does not explain the smallness of neutrino masses compared to other particles [21].

In particular, Majorana masses can arise through the seesaw mechanism, being an economic possibility as do not require for the existence of right handed neutrinos.

Type-II seesaw mechanism

Seesaw of type II [5, 6, 22–24] requires for an extension of the scalar sector by a scalar triplet with hypercharge $y_\delta = 2$. In this model, lepton number is broken explicitly in the scalar potential by a trilinear coupling, μ, as discussed already in Section 2.

The $\mathcal{L}_{\mathrm{Y}}$ term in (2.1) contains all the Yukawa sector, being that of the SM plus the extra Yukawas coupling the $SU(2)_L$ doublets with the Higgs triplet. The new Yukawa term leads to a Majorana mass terms for neutrinos once the neutral component of Δ acquires a vacuum expectation value (vev), v_δ, without requiring right-handed neutrino states. The Yukawa Lagrangian can be defined as follows:

$$\mathcal{L}_{\mathrm{Y}} = \mathcal{L}_{\mathrm{Y}}^{\mathrm{SM}} - \left[(Y_v)_{ij}\, L_i^T C i\sigma_2 \Delta L_j + \mathrm{h.c.} \right], \tag{2.56}$$

denoting by L the $SU(2)_L$ doublets of left-handed leptons, Y_v denotes the Yukawa couplings of the lepton doublets with the triplet fields and C the charge conjugation operator. This term can be rewritten in terms of the neutrino masses as:

$$-(Y_v)_{ij}\, L_i^T C i\sigma_2 \Delta L_j + \mathrm{h.c.} = -\frac{(M_v)_{ij}}{\sqrt{2} v_\delta} L_i^T C i\sigma_2 \Delta L_j + \mathrm{h.c.}, \tag{2.57}$$

from where it can be easily derived:

$$\mathcal{L}_{\mathrm{Y}}^{m^{(\nu)}} = -\frac{1}{2}\, (M_v)_{ij} \left(\bar{\nu}_{L,i}^c \nu_{L,j} + \bar{\nu}_{L,i} \nu_{L,j}^c \right) \tag{2.58}$$

where $M_v = U m_v U^\dagger$ is the neutrino mass matrix in the basis where the charged lepton masses are diagonal. m_v stands for the neutrino masses and U is the would be Pontecorvo-Maki-Nakagawa-Sakata matrix. It is evident that the Majorana mass term violates Lepton number in two units.

Being the neutrino masses defined in terms of the Yukawa couplings as $(M_v)_{ij} = \sqrt{2} v_\delta \, (Y_v)_{ij}$, from Equation (2.30) it follows that in the $M \gg v$ limit, the type II seesaw mechanism will produce neutrino masses of order:

$$m_v \sim y \frac{\mu v_\phi^2}{M^2}, \tag{2.59}$$

where y corresponds to the Yukawa couplings in the neutrino mass basis. The trilinear coupling μ breaks lepton number and thus can be protected by symmetry and be naturally small. Therefore, neutrinos can be supposed to be light compared to the electroweak scale for triplet masses around the TeV.

Another interesting feature of the model is the possibility of testing neutrino parameters from decays in the leptonic sector. The couplings between the scalar and leptonic sectors will be presented in the following Section while the scalars decays into leptons will be discussed later in Section 3.4.

2.5 Implications for the leptonic sector

The introduction of new scalar into the particle content of the theory will lead to new interactions, not only with gauge bosons but also in the leptonic sector. These new scalar-leptons interactions, that are introduced as Yukawa terms in the Lagrangian as occurred for the Higgs boson within the SM, will be obtained in this Section.

From the Yukawa Lagrangian in Equation (2.56):

$$-\,(Y_v)_{ij}\, L_i^T C i\sigma_2 \Delta L_j + \text{h.c.} = -\frac{(Y_v)_{ij}}{\sqrt{2}} \begin{pmatrix} -\bar{\ell}^c_{L,i} & \bar{\nu}^c_{L,i} \end{pmatrix} \begin{pmatrix} \omega_\delta^+ & \sqrt{2}\,\delta^{++} \\ v_\delta + h_\delta + i\eta_\delta & -\omega_\delta^+ \end{pmatrix} \begin{pmatrix} \nu_{L,j} \\ \ell_{L,j} \end{pmatrix} + \text{h.c.}, \tag{2.60}$$

where all the fields in (2.60) are left handed as the triplet fields do not couple with right handed fields. Expanding, in terms of the triplet fields, the following is obtained:

$$\begin{aligned} -\,(Y_v)_{ij}\, L_i^T C i\sigma_2 \Delta L_j + \text{h.c.} = &-\frac{(Y_v)_{ij}}{\sqrt{2}} \Big[\bar{\nu}^c_{L,i} \nu_{L,j} \left(v_\delta + h_\delta + i\eta_\delta \right) - \left(\bar{\ell}^c_{L,i} \nu_{L,j} + \bar{\nu}^c_{L,i} \ell_{L,j} \right) \omega_\delta^+ \\ &- \sqrt{2}\, \bar{\ell}^c_{L,i} \ell_{L,j}\, \delta^{++} \Big] + \text{h.c.} \end{aligned} \tag{2.61}$$

After some computation, the total Yukawa interactions in term of the physical fields can be summarised as follows. For the neutral currents:

$$\begin{aligned} \mathcal{L}_{\rm Y}^{\text{neutral}} = &-\frac{m_i^{(\ell)}}{v_\phi} \bar{\ell}_i \ell_i \left(c_\alpha h - s_\alpha H \right) - \frac{m_i^{(\nu)}}{2 v_\delta} \bar{\nu}_i \nu_i \left(s_\alpha h + c_\alpha H \right) \\ &- i \frac{m_i^{(\ell)}}{v_\phi} \bar{\ell}_i \gamma_5 \ell_i s_\tau \theta - i \frac{m^{(\nu)_i}}{2 v_\delta} \bar{\nu}_i \gamma_5 \nu_i c_\tau \theta, \end{aligned} \tag{2.62}$$

where the ℓ_i and ν_i are the leptonic mass eigenstates, that have been defined as in [17], i.e.:

$$\ell = S_1 \left(\ell_L + V_1 \ell_R\right), \tag{2.63}$$
$$\nu = S_2 \left(V_2 \nu_L - \nu_L^c\right), \tag{2.64}$$

being V_i defined as $V_i = \sqrt{2}/v_i \, H_i^{-1} Y^i$, where H_i is an hermitian matrix whose diagonalization $H_i = S_i^\dagger D_i S_i$ gives the diagonal mass matrix D_i. Here, the index $i = 1$ correspond to the charged leptons and $i = 2$ is used for neutrinos.

Now, for the charged currents:

$$\begin{aligned}\mathcal{L}_{\mathrm{Y}}^{\text{charged}} =& \Big[-\sqrt{2}\,(Y_v)_{ij}\,\bar{\ell}^c_{L,i}\nu_{L,j} c_\beta H^+ - (Y_0)_{ij}\,\bar{\nu}_{L,i}\ell_{R,j}\, s_\beta H^+ \\ &+ (Y_v)_{ij}\,\bar{\ell}^c_{L,i}\ell_{L,j}\,\delta^{++}\Big] + \text{h.c.}\,,\end{aligned} \tag{2.65}$$

In this model the mass term of the charged leptons does not change and therefore remains as in the SM.

For the neutral terms, as the scalar fields couple with leptons in their mass eigenstates basis (in the same way as the vevs), then there won't be any FCNC appearing at tree level. From the charged interaction it can be seen that $L = 2$ interactions have to be considered in this model, these new interactions are shown in Figure 2.1.

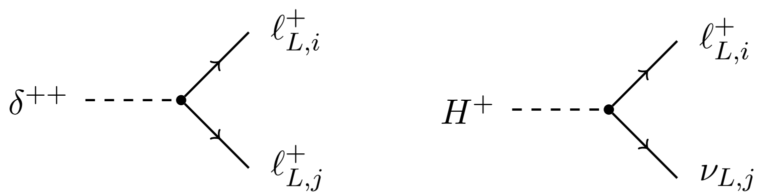

Figure 2.1: *Feynman diagrams associated with processes with $L = 2$ within the Higgs triplet model.*

Now that the model has been introduced and some theoretical constraints and interactions have been discussed the phenomenology of the model will be analysed.

3 Phenomenology of the HTM

In this Chapter, a discussion of some of the phenomenological implications of adding a scalar triplet with hypercharge $y_\delta = 2$ to the SM particle content will be performed. First, in Section 3.1 the allowed parameter space will be computed using the arguments of unitarity, BFB and the absence of tachyonic modes, summarised in Section 2.3. The one loop corrections to the electroweak parameters will be the topic of Section 3.2. In Section 3.3, the light Higgs decay into photons will be analysed. Finally, the phenomenology of the triplet-like particle decays will be explored in Section 3.4.

3.1 The parameter space in the HTM

To begin with, the parameters of the scalar potential can be traded to the physical masses and the vacuum expectation values in order to obtain meaningful understanding from Eqs. (2.39 - 2.52). This has been done as in [20], giving the relations:

$$\mu = \frac{\sqrt{2}v_\delta}{v_\phi^2 + 4v_\delta^2} m_\theta^2 \,, \tag{3.1}$$

$$\lambda = \frac{2}{v_\phi^2}\left(s_\alpha^2 m_H^2 + c_\alpha^2 m_h^2\right) \,, \tag{3.2}$$

$$\lambda_1 = \frac{4}{v_\phi^2 + 2v_\delta^2} m_{H^+}^2 - \frac{2}{v_\phi^2 + 4v_\delta^2} m_\theta^2 - \frac{s_\alpha c_\alpha}{v_\phi v_\delta}\left(m_H^2 - m_h^2\right) \,, \tag{3.3}$$

$$\lambda_2 = \frac{1}{v_\delta^2}\left[\frac{1}{2}\left(s_\alpha^2 m_h^2 + c_\alpha^2 m_H^2\right) + \frac{v_\phi^2}{2(v_\phi^2 + 4v_\delta^2)} m_\theta^2 - \frac{2v_\phi^2}{v_\phi^2 + 2v_\delta^2} m_{H^+}^2 + m_{\delta^{++}}^2\right] \,, \tag{3.4}$$

$$\lambda_3 = \frac{1}{v_\delta^2}\left[\frac{2v_\phi^2}{v_\phi^2 + 2v_\delta^2} m_{H^+}^2 - \frac{v_\phi^2}{v_\phi^2 + 4v_\delta^2} m_\theta^2 - m_{\delta^{++}}^2\right] \,, \tag{3.5}$$

$$\lambda_4 = \frac{4}{v_\phi^2 + 4v_\delta^2} m_\theta^2 - \frac{4}{v_\phi^2 + 2v_\delta^2} m_{H^+}^2 \,. \tag{3.6}$$

The parameters m_Φ^2 and M^2 can be easily exchanged to the physical parameters through the Eqs. (2.10, 2.11). To complete the determination in terms of physical quantities one should further deduce the mixing angle α from the measurement of some couplings and the values of v_ϕ and v_δ. The

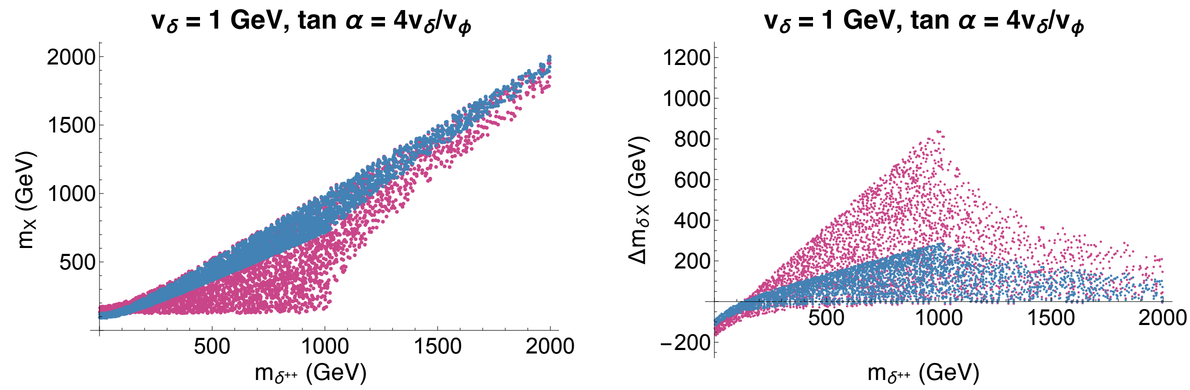

Figure 3.1: *In the left figure, the allowed values for the masses of the particles of the model, m_{H^+} (blue) and m_θ (pink), as a function of the mass $m_{\delta^{++}}$ are shown. The right figure shows the results from the computation of the mass difference $\Delta m_{\delta X} \equiv m_{\delta^{++}} - m_X$ with $X = H^+$ (blue) and $X = \theta$ (pink). Both Figures have been computed using nothing else but arguments of unitarity, vacuum stability and the absence of tachyonic modes.*

vev of the model v_ϕ and v_δ could be expressed in terms of observables. One option would be to replace them for m_Z, m_W and c_W as

$$v_\phi^2 = \frac{s_W^2}{\pi \alpha_{\text{QED}}}(2m_W^2 - c_W^2 m_Z^2) \, , \qquad v_\delta^2 = \frac{s_W^2}{2\pi \alpha_{\text{QED}}}(c_W^2 m_Z^2 - m_W^2), \tag{3.7}$$

where the dependence on the deviance of the ρ parameter from unity is present, this will be discussed in depth later in Section 3.2. Some other possibilities are contained in [20].

For the computation of the allowed parameter space the approximate expression of s_α from (2.31) will be used. This should be taken into account when analysing the results for values of $m_{\delta^{++}} < 500$ GeV, as the results shown here should not be fully reliable in this energy region. Even so, s_α would be small in any case because of the constraint coming from the ρ parameter.

In here, the masses of the particles ($m_{\delta^{++}}$, m_{H^+}, m_θ, m_H and m_h) and the vev of the triplet (v_δ, or s_α) are taken to be the d.o.f. of the model. From that, all the parameters of the model can be obtained. For the results that appear in this work the input value $v_\delta = 1$ GeV has been fixed, although some other values have been used to check that there are no meaningful changes appearing. Here, the assumption $m_H, m_\theta > m_h$ will be made although the other configuration is still allowed by the data (depending on the value of v_δ). This assumption would be necessary to avoid Higgs and gauge bosons decay into these particles.

The computation has been done and the results for the masses of the θ, H^+ and δ^{++} and the mass difference $\Delta m_{\delta X} \equiv m_{\delta^{++}} - m_X$ ($X = \theta$, H^+. The notation $\Delta m_{XY} = m_X - m_Y$ will be used from now on) are shown in Figure 3.1. It can be seen for values of $m_{\delta^{++}} > 500$ GeV that the parameter space seems to favour the massive particle of the model to be δ^{++}, although the degenerate configuration of $m_{\delta^{++}} \simeq m_{H^+} \simeq m_\theta$ and the inverse mass hierarchy are allowed.

This "preference" on δ^{++} being the heavier particle of the model could be understood from λ_4 being smaller than zero as well as H^+ being heavier than θ (the mass difference $\Delta m_{H^+\theta}$ also depends on λ_4, as stated in Section 2.2). This has been checked and the results are shown in Figure 3.2. The same behaviour is found for the mass difference $\Delta m_{H^+\theta}$.

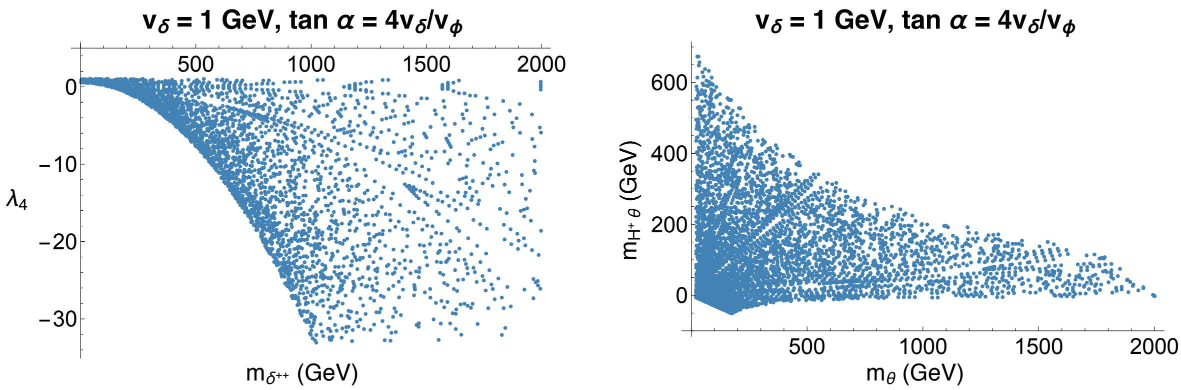

Figure 3.2: *In the left figure, the parameter λ_4 is shown as a function of $m_{\delta^{++}}$ for the input values of $v_\delta = 1$ GeV and $\tan\alpha = 4v_\delta/v_\phi$. The right figure shows the mass difference $\Delta m_{H^+\theta} \equiv m_{H^+} - m_\theta$. Both Figures have been computed using nothing else but arguments of unitarity, vacuum stability and the absence of tachyonic modes.*

In Figure 3.3 (left) the quantity $\Delta m_{\delta H^+} - \Delta m_{H^+\theta} = m_{\delta^{++}} + m_\theta - 2m_{H^+}$, which gives a measure for the difference of the splitting between the masses of the δ^{++} and H^+ and the H^+ and θ particles respectively, is plotted. This figure shows that the parameter space of the model allows for a degenerate spectrum of the heavy particles masses. In the region $m_{\delta^{++}} \in (1, 1000)$ GeV both configurations for the mass splitting are allowed ($m_{\delta^{++}} - m_{H^+} \simeq m_{H^+} - m_\theta$ and $m_{\delta^{++}} - m_{H^+} \neq m_{H^+} - m_\theta$). More interesting is the case of $m_{\delta^{++}} > 1$ TeV, where only the possibility of $m_{\delta^{++}} - m_{H^+} \simeq m_{H^+} - m_\theta$ remains. In this case the splitting has an upper bound of ~ 200 GeV, as can be seen from Figure 3.1, i.e. the splitting does not exceed a $10 - 20\%$ of the value of $m_{\delta^{++}}$. This mass splitting would be strongly constrained later, once the corrections to the oblique parameter T are introduced.

Additionally, one interesting relation can be obtained by inserting Equations (3.4) and (3.5) into Equation (2.48.10), as done in [21]

$$0 \leq \left(s_\alpha^2 m_h^2 + c_\alpha^2 m_H^2\right) - \frac{v_\phi^2\, m_\theta^2}{v_\phi^2 + 4v_\delta^2} \leq 16\pi v_\delta^2 \,. \tag{3.8}$$

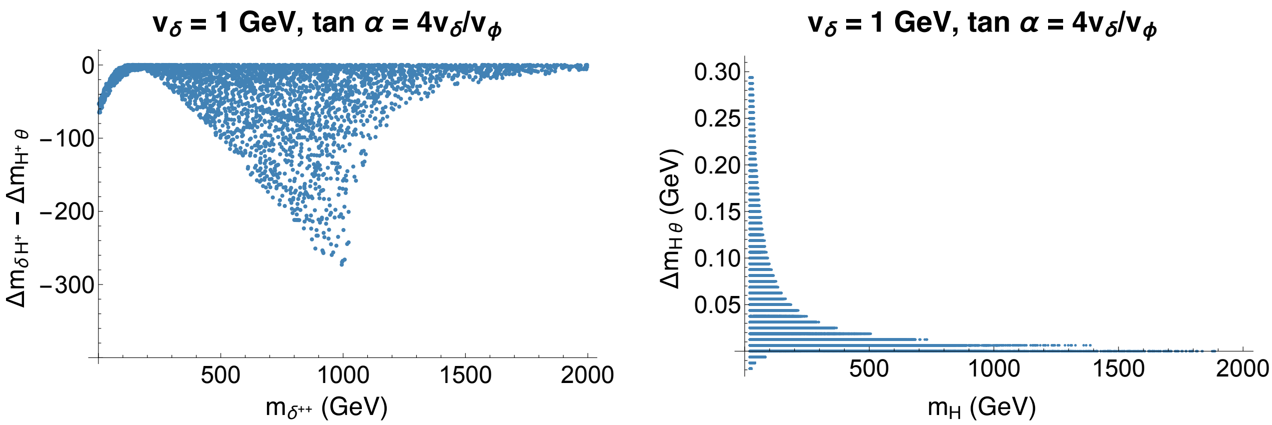

Figure 3.3: *In the left figure, the difference of the splitting between the heavy particles $\Delta m_{\delta H^+} - \Delta m_{H^+\theta} = m_{\delta^{++}} + m_\theta - 2m_{H^+}$ of the HTM is shown. The right figure shows the mass difference $\Delta m_{H\theta} \equiv m_H - m_\theta$. Both Figures have been computed using nothing else but arguments of unitarity, vacuum stability and the absence of tachyonic modes.*

Doing some simplifications:

$$(1-\xi)\, m_\theta^2 \leq (1-\xi)\, m_H^2 \leq (1-\xi)\, m_\theta^2 + 16\pi v_\delta^2, \tag{3.9}$$

where $\xi = 4v_\delta^2/v_\phi^2$. Thus, (3.9) leads to the following relation:

$$m_\theta^2 \lesssim m_H^2 \lesssim m_\theta^2 + 16\pi v_\delta^2. \tag{3.10}$$

This relation has been checked and is shown in Figure 3.3 (right). Therefore, the masses of the H and θ scalars are the same up to some tiny corrections $\mathcal{O}(v_\delta^2/v_\phi^2)$.

3.2 One loop corrections to electroweak parameters

As commented in the introduction, the ρ parameter imposes major constraints for all the scalar extensions of the SM other than singlets or doublets with $y = 1$. In Equation (2.9), it was shown that the HTM introduced a deviation of the ρ parameter with respect to the prediction of the SM, which was parametrized as $\delta\rho = -2\,\alpha^2$, i.e. the deviation from $\rho = 1$ was proportional to v_δ^2/v_ϕ^2 at tree level.

The one-loop corrected electroweak observables relevant to the HTM have been computed in [7] for the same model as in this work and in [25] for a HTM with hypercharge $y_\delta = 0$. The on-shell scheme was used in both cases. The computation of the corrected electroweak observables is necessary for two main reasons: to begin with, it should be checked that corrections to the ρ parameters do not imply a strong deviation from the experimental value, even for the SM. The second reason is that as new particles have been introduced to the particle content of the SM new corrections are to be taken into account and those should be compared with the corrections induced within the SM. Therefore, by looking at how the properties of these new particles produce deviations from the SM observables, new constraints on the parameter space of the model will arise.

In the SM, and in models with $\rho = 1$ at the tree level, all the electroweak parameters can be determined from a set of three input parameters, one useful example would be the set: α_{em}, G_F and m_Z, being the values of those parameters well known experimentally. On the other hand, for models with $\rho \neq 1$ at the tree level like the HTM, an additional input parameter is necessary to fully determine all the electroweak parameters, i.e., in addition to α_{em}, G_F and m_Z, another parameter as the weak angle $\sin^2\theta_W$ should be chosen as the fourth input, as done in [7, 25].

Using the same values of these input parameters as in refs. [7, 25], from [26]

$$\begin{aligned} &\alpha_{\text{em}}^{-1}(m_Z) = 128.903(15), && G_F = 1.1663787(6)\times 10^{-5}\ \text{GeV}^{-2}, \\ &m_Z = 91.1876(21)\ \text{GeV}, && \hat{s}_W^2(m_Z) = 0.23146(12), \end{aligned} \tag{3.11}$$

where $\hat{s}_W^2 \equiv \hat{s}_W^2(m_Z)$ ($\hat{c}_W^2 = 1 - \hat{s}_W^2$) is defined as the ratio of the coefficients of the vector part and the axial vector part in the $Z\bar{e}e$ vertex:

$$1 - 4\hat{s}_W^2(m_Z) = \frac{\text{Re}(v_e)}{\text{Re}(a_e)}, \tag{3.12}$$

being v_e and a_e defined as:

$$v_e = -\frac{1}{2} + 2\hat{s}_W^2 \qquad\qquad a_e = -\frac{1}{2}\,. \tag{3.13}$$

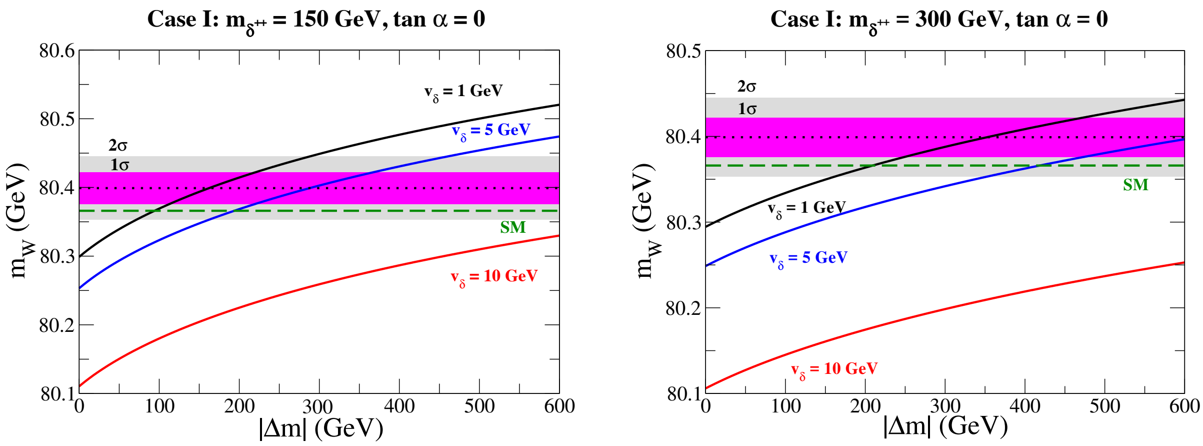

Figure 3.4: *The one-loop corrected values of m_W as a function of the absolute value of Δm and for different values of v_δ in Case I ($m_\theta > m_{H^+} > m_{\delta^{++}}$). The values $m_h = 125$ GeV, $m_t = 173$ GeV and $\tan\alpha = 0$ have been used for both figures. The pink (gray) shaded region represents the 1σ (2σ) error for the experimental data of $m_W^{exp} = 80.399 \pm 0.023$ GeV [26]. In the left (right) figure, the mass of the lightless scalar has been taken to be $m_{\delta^{++}}$ = 150 GeV (300 GeV). The dashed green line shows the SM prediction of m_W at the one-loop level with a SM Higgs boson with mass $m_h = 125$ GeV. These Figures have been taken from [7].*

Therefore, the expression of m_W^2 and ρ in terms of the four input parameters [7]:

$$m_W^2 = \frac{\pi\alpha_{\text{em}}}{\sqrt{2}G_F\hat{s}_W^2}(1+\Delta r), \qquad \rho = \frac{\pi\alpha_{\text{em}}}{\sqrt{2}G_F\hat{s}_W^2\hat{c}_W^2 m_Z^2}(1+\Delta r), \tag{3.14}$$

where the radiative corrections have been parametrized by the factor Δr. Therefore, in terms of four input parameters, Δr determines both the one-loop corrected mass of the W boson and the ρ parameter in the HTM. Δr is given by [7].

$$\Delta r = \frac{\Pi_T^{WW}(0) - \Pi_T^{WW}(m_W^2)}{m_W^2} + \frac{d}{dp^2}\Pi_T^{\gamma\gamma}(p^2)\Big|_{p^2=0} + \frac{2\hat{s}_W}{\hat{c}_W}\frac{\Pi_T^{\gamma Z}(0)}{m_Z^2} - \frac{\hat{c}_W}{\hat{s}_W}\frac{\Pi_T^{\gamma Z}(m_Z^2)}{m_Z^2} + \delta_{VB} + \delta_V'. \tag{3.15}$$

In (3.15), δ_{VB} and δ_V' are the vertex and the box diagram corrections to G_F and the radiative corrections to the $Z\bar{e}e$ vertex, respectively. $\Pi_T^{XY}(p^2)$ $(X, Y = W, Z, \gamma)$ are the 1PI diagrams for the gauge boson self-energies. The analytic expressions for the gauge boson self-energies in the HTM with the $y_\delta = 2$ triplet field have been computed and can be found in [7].

These corrections depend on the mass spectrum and the doublet-triplet mixing angle; i.e., $m_{\delta^{++}}$, m_{H^+}, m_θ, m_H, m_h and $\tan\alpha$. In [7], the mass m_{H^+} is traded for the mass difference $\Delta m_{\delta H^+} = m_{\delta^{++}} - m_{H^+}$ and the splitting $m_{\delta^{++}}^2 - m_{H^+}^2 \approx m_{H^+}^2 - m_\theta^2$ discussed in (2.37) is assumed. There should not be any problem with this assumption when going to masses around the TeV, but it is evident by looking at Figures 3.1 and 3.2 that for $m_{\delta^{++}}$, $m_\theta < 1$ TeV the contributions from λ_3 and the factor μv_δ will have a main importance for the mass of these particles at those scales, where the behaviour $m_{\delta^{++}}^2 - m_{H^+}^2 \approx m_{H^+}^2 - m_\theta^2$ can not be ensured (see Figure 3.3 - left). Even though the configuration from [7] is not the most general, it is contained within the allowed parameter space of the model and therefore it will be analysed taking this into account. As well, it should be noted that for many of the

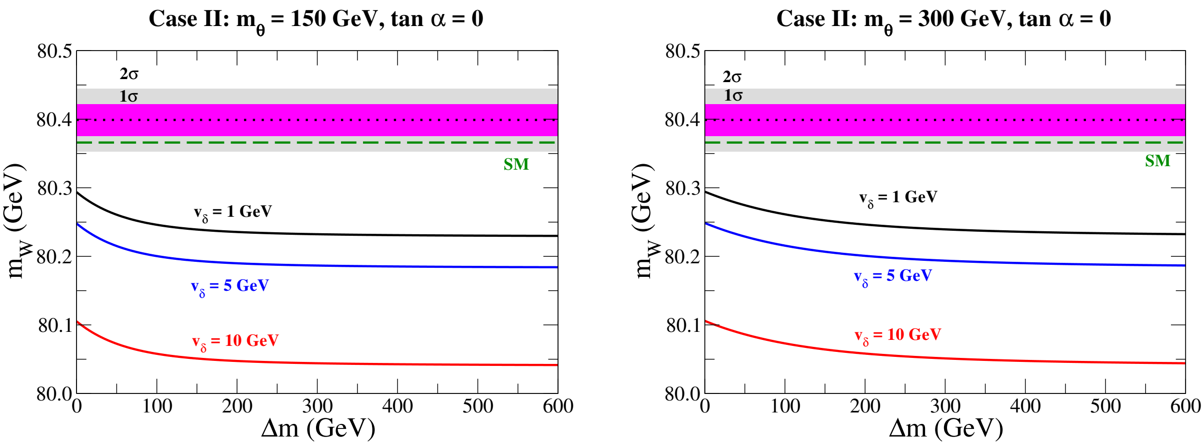

Figure 3.5: *The one-loop corrected values of m_W as a function of the absolute value of Δm and for different values of v_δ in Case II ($m_{\delta^{++}} > m_{H^+} > m_\theta$). The values $m_h = 125$ GeV, $m_t = 173$ GeV and $\tan\alpha = 0$ have been used for both figures. The pink (gray) shaded region represents the 1σ (2σ) error for the experimental data of $m_W^{exp} = 80.399 \pm 0.023$ GeV [26]. In the left (right) figure, the mass of the lightless scalar has been taken to be m_θ = 150 GeV (300 GeV). The dashed green line shows the SM prediction of m_W at the one-loop level with a SM Higgs boson with mass $m_h = 125$ GeV. These Figures have been taken from [7].*

results presented by [7] the parameter s_α has been set to be zero. This limit is in fact excluded, as noted by [21] and as will be shown later in Section 3.3. Even though, the results should not differ notably for the computation of the correction to m_W and ρ as the differences on the couplings between gauge bosons and scalars do not depend strongly on this variation [7]. This will be commented later in Section 3.3. In this Section, the notation $\Delta m \equiv \Delta m_{\delta H^+} = \Delta m_{H^+\theta}$ will be used.

The results for the two scenarios for the mass splitting analysed in [7] are presented. A mass of the top quark of $m_t = 173$ GeV and $m_b = 4.7$ GeV for the bottom quark have been used. Leading order QCD corrections have been taken into account with a value of $\alpha_s(m_Z) = 0.118$ [7]. The numerical results of the one-loop corrected values of m_W as a function of the absolute value of Δm and for different values of v_δ for Case I ($m_\theta > m_{H^+} > m_{\delta^{++}}$) for a mass of $m_{\delta^{++}} = 150$ GeV (left) and $m_{\delta^{++}} = 300$ GeV (right) are shown in Figure 3.4. $\tan\alpha$ has been taken to be equal to zero. The pink (gray) shaded region represents the 1σ (2σ) error for the experimental data of $m_W^{\text{exp}} = 80.399 \pm 0.023$ GeV [26]. The dashed green line shows the SM prediction of m_W at the one-loop level with a SM Higgs boson with mass $m_h = 125$ GeV.

It can be seen that for Case I the degenerate configuration ($\Delta m = 0$) is excluded for all values of v_δ (the behaviour for $v_\delta < 1$ GeV does not differ for the one presented at $v_\delta = 1$ GeV [7]). The favoured splitting would be of $70 - 80 \lesssim |\Delta m| \lesssim 300$ for $v_\delta = 1$ GeV and $160 \lesssim |\Delta m| \lesssim 460$ for $v_\delta = 5$ GeV for the input value $m_{\delta^{++}} = 150$ GeV. For a larger value of $m_{\delta^{++}}$ (right) the allowed range of the splitting becomes larger and wider being $160 \lesssim |\Delta m| \lesssim 600$ for $v_\delta = 1$ GeV and $360 \lesssim |\Delta m|$ for $v_\delta = 5$ GeV. Even still, the degenerate case is not allowed for this configuration. The limits set on $|\Delta m|$ from perturbative unitarity are found around ~ 400 GeV for Case I and for ~ 1 TeV for Case II.

The same analysis has been performed by [7] for Case II ($m_{\delta^{++}} > m_{H^+} > m_\theta$) for a mass of $m_\theta = 150$ GeV and $m_\theta = 300$ GeV. Results are shown in Figure 3.5 and the same conditions and input parameters from Case I have been used. For θ being the lightless of the triplet-like particles there is no configuration of v_δ and Δm compatible with the experimental measurements of m_W, neither for $m_\theta = 150$ GeV (left) nor $m_\theta = 300$ GeV (right). This Case is therefore clearly disfavoured by the

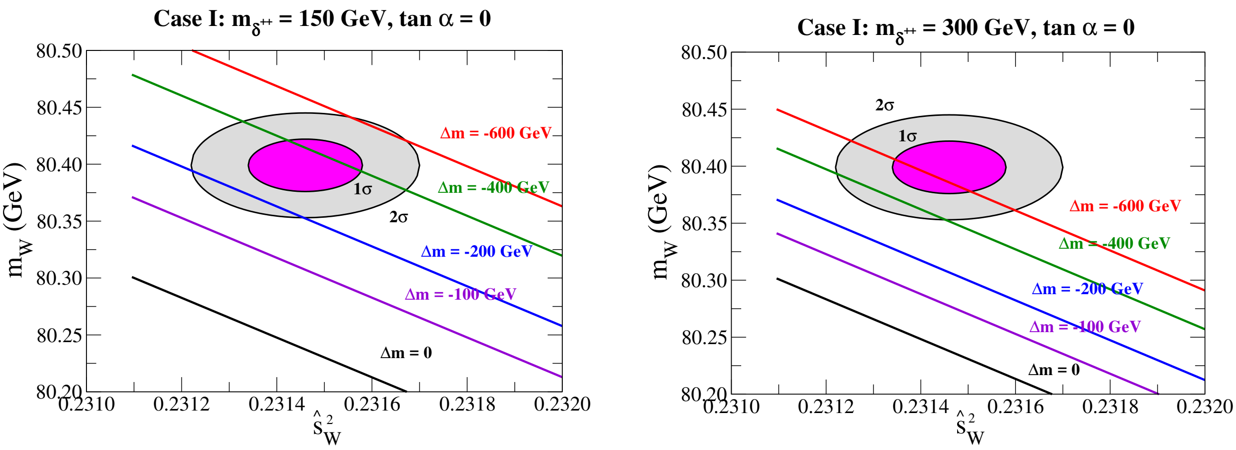

Figure 3.6: *The one-loop corrected values of m_W as a function of $\hat{s}^2_W$ and for different values of Δm in Case I ($m_\theta > m_{H^+} > m_{\delta^{++}}$). The values $m_h = 125$ GeV, $m_t = 173$ GeV and $\tan\alpha = 0$ have been used for both figures. The pink (gray) shaded region represents the 1σ (2σ) error for the experimental data of $m_W^{exp} = 80.399 \pm 0.023$ GeV and $\hat{s}^2_{W,\,exp} = 0.23146 \pm 0.00012$ GeV [26]. In the left (right) figure, the mass of the lightless scalar has been taken to be $m_{\delta^{++}} =$ 150 GeV (300 GeV). These Figures have been taken from [7].*

electroweak precision data coming from m_W.

Therefore, from Figures 3.4 and 3.5 Case I results as favoured from the experimental constraints of m_W. Now, the study can be extended for both cases and the renormalized value of m_W has been computed as function of $\hat{s}^2_W$, for different values of Δm. Again, the same input parameters such as the bottom and top quark masses, $\tan\alpha$ and m_h have been used.

Figure 3.6 shows the renormalized values of m_W as a function of $\hat{s}^2_W$ for different values of Δm. The pink (gray) shaded region represents the 1σ (2σ) error for the experimental data of $m_W^{\text{exp}} = 80.399 \pm 0.023$ GeV and $\hat{s}^2_{W,\,\text{exp}} = 0.23146 \pm 0.00012$ GeV [26]. It can be seen that the degenerate case is not included within the allowed data for none of the cases. For $m_{\delta^{++}} = 150$ GeV (left), the data will agree with values of $-600 \lesssim \Delta m \lesssim -160$ GeV. The bound for the coloured lines correspond with the limit of $v_\delta = 0$, which can be computed by defining v_δ in terms of the four input parameters as:

$$v_\delta^2 = \frac{\hat{s}^2_W \hat{c}^2_W}{2\pi\alpha_{\text{em}}} m_Z^2 - \frac{\sqrt{2}}{4G_F}, \tag{3.16}$$

and taking v_δ to zero.

For $m_{\delta^{++}} = 300$ GeV (right), the data will require larger values of Δm compared to those from the left figure. In this case the allowed range will be of $-600 \lesssim \Delta m \lesssim -300$ GeV. For $m_{\delta^{++}} = 300$ GeV the predicted values of m_W are smaller for the same value of Δm (for a non-zero value) than they were for the left figure, i.e. smaller values of $m_{\delta^{++}}$ will predict larger values of m_W (for the same splitting). In the limit Δm going to 0 the prediction remains the same.

In Figure 3.7 the computation has been repeated considering now the CP-odd scalar, θ, to be the lightest. The input masses $m_\theta = 150$ GeV (left) and $m_\theta = 300$ GeV have been used (right) and the input parameters remain the same as used for Figures 3.4, 3.5 and 3.6.

As happened in Figure 3.5, there is no region of data compatible with θ being the lightest of the triplet-like scalars. In this case the highest value for the m_W mass is found for $\Delta m = 0$, but happens to

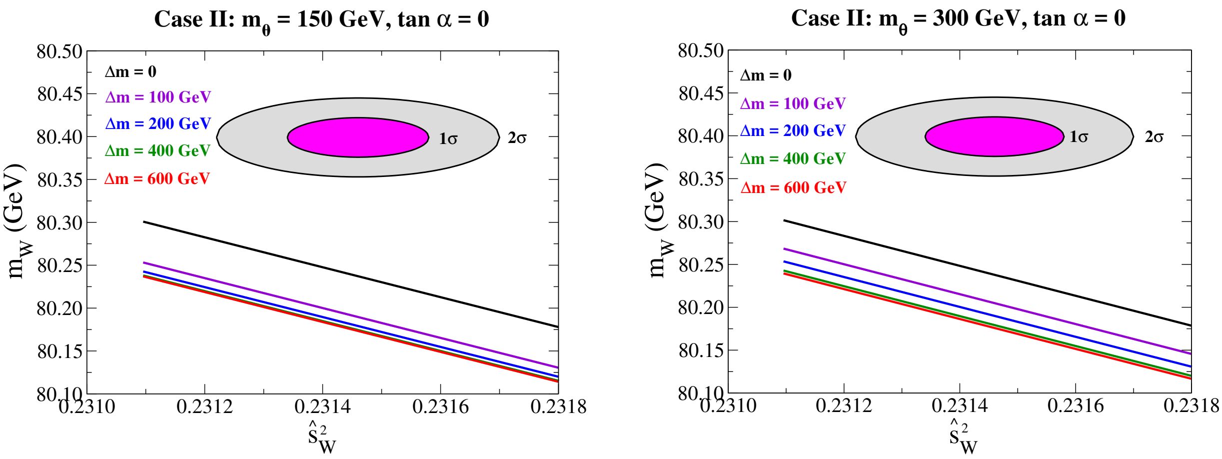

Figure 3.7: *The one-loop corrected values of m_W as a function of $\hat{s}_W^2$ and for different values of Δm in Case II ($m_{\delta^{++}} > m_{H^+} > m_\theta$). The values $m_h = 125$ GeV, $m_t = 173$ GeV and $\tan\alpha = 0$ have been used for both figures. The pink (gray) shaded region represents the 1σ (2σ) error for the experimental data of $m_W^{exp} = 80.399 \pm 0.023$ GeV and $\hat{s}^2_{W,\,exp} = 0.23146 \pm 0.00012$ GeV [26]. In the left (right) figure, the mass of the lightless scalar has been taken to be m_θ = 150 GeV (300 GeV). These Figures have been taken from [7].*

be out of the allowed region. Again, Case I is favoured by the experimental constraints, now from m_W and $\hat{s}_W^2$ precision data.

Now the study will be focused on the one loop corrections to the ρ parameter as a function of v_δ, from Equation (3.14). The input parameters will remain the same and the values $m_h = 125$ GeV, $m_t = 173$ GeV and $\tan\alpha = 0$ have been used. The deviation from the SM prediction will be parametrised as $\Delta\rho \equiv \rho - \rho_{\rm SM}(m_h)$ [7]. The experimental deviation was computed in [7] using the data of the oblique T parameter from [26], being $\Delta\rho^{\rm exp} = 0.000632 \pm 0.000621$. Results are shown in Figure 3.8 for Case I (left) and Case II (right) for different values of Δm.

As occurred in the study of m_W, the degenerate case is not allowed by the data, neither for Case I nor Case II. Case I is in agreement with Δm being around $\sim (-400, -100)$ GeV for a value of v_δ of $\sim 3.5 - 8$ GeV, coinciding with the results obtained from Figure 3.4. Case II is clearly disfavoured by the electroweak precision data of $\Delta\rho$, as occurred to be for m_W, as Figure 3.8 shows that there is no possible configuration of v_δ and Δm contained within the 2σ region.

The results of the deviation of the ρ parameter prediction within the HTM with the SM as a function of the mass of the lightless triplet-like scalar are included in Figure 3.9, where now a non zero value of $\tan\alpha$ is used (previous results from Figure 3.8 encourages to set v_δ around 5 GeV). For this computation a new parameter, $\xi \equiv m^2_{\delta^{++}} - m^2_{H^+}$, has been defined and values from 100 GeV to 3 TeV have been considered. In this case, the limit of $m_{\rm lightless}$ going to infinity has been assumed and $\tan\alpha$ has been set to be $\tan\alpha = 2v_\delta/v$.

It can be seen that the results support values of $m_{\rm lightlest}$ at the GeV order, for values of ξ of $(-500^2, -100^2)$ GeV^2. The Case II configuration is (once again) out of the 2σ region and therefore, this mass hierarchy for the HTM (for this configuration of masses) could be considered as excluded. The allowed values for ξ have been computed using the results from Section 3.1, being its maximum value of ~ 700 GeV.

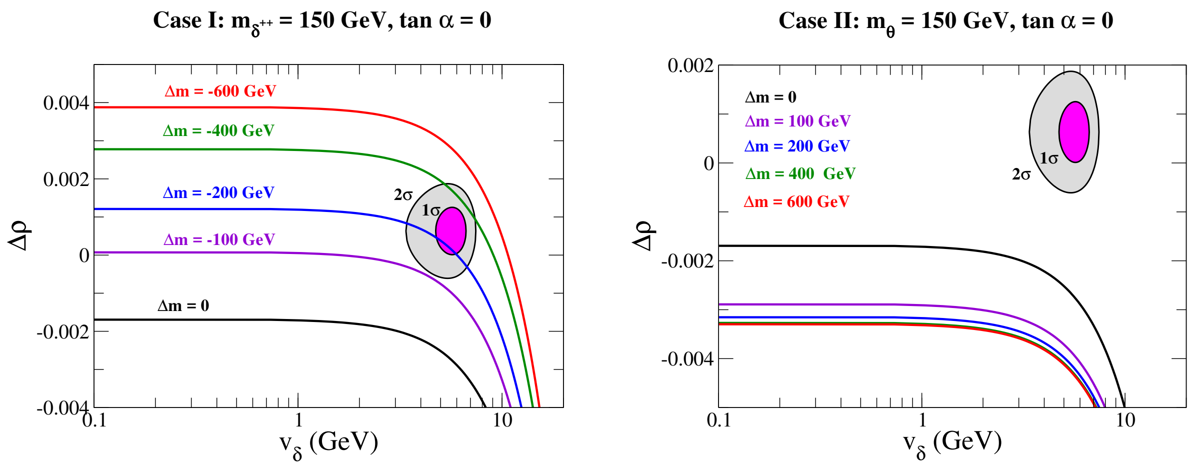

Figure 3.8: *The one-loop corrected value deviation of $\Delta\rho$ from the ones predicted by the SM, as a function of v_δ and for different values of Δm. The values $m_h = 125$ GeV, $m_t = 173$ GeV and $\tan\alpha = 0$ have been used for both figures. The pink (gray) shaded region represents the 1σ (2σ) error for the experimental data of $\Delta\rho^{exp} = 0.000632 \pm 0.000621$ which has been computed by [7], derived from the data of the T parameter ($T = 0.07 \pm 0.08$) [26]. In the left figure, Case I ($m_\theta > m_{H^+} > m_{\delta^{++}}$) is considered, with $m_{\delta^{++}} = 150$ GeV. In the right figure, the results for Case II ($m_{\delta^{++}} > m_{H^+} > m_\theta$) are shown, and m_θ is fixed at 150 GeV. These Figures have been taken from [7].*

The fact of $\Delta\rho$ not coinciding with the SM prediction in the limit of m_{lightest} going to infinity, when the theory decouples, comes from the choice of parameters. Without imposing $m_W = m_Z c_W$ the predictions differs as in [7] four input parameters have been used while the predictions within the SM are computed using three of them plus the tree level relation $m_W = m_Z\, c_W$.

For a better understanding of the phenomenological implications for this model, the study of the corrected electroweak parameters should be performed allowing all the possible configurations for any

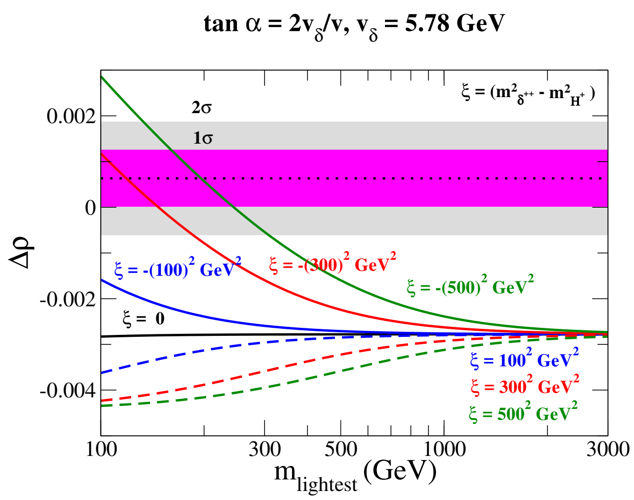

Figure 3.9: *Deviation of the ρ parameter prediction within the HTM and the SM as a function of the mass of the lightless triplet-like scalar (m_{lightest}) for different values of $\xi \equiv m^2_{\delta^{++}} - m^2_{H^+}$. The values $m_h = 125$ GeV, $m_t = 173$ GeV and $v_\delta = 5.78$ GeV ($\tan\alpha = 2v_\delta/v$) have been used. The pink (gray) shaded region represents the 1σ (2σ) error for the experimental data of $\Delta\rho^{exp} = 0.000632 \pm 0.000621$ which have been obtained from the data of the T parameter ($T = 0.07 \pm 0.08$ [26]). This Figure has been taken from [7].*

set of degrees of freedom. There is no reason a priori to cut down from the three $m_{\delta^{++}}$, m_{H^+} and m_θ parameters down to only $m_{\delta^{++}}$ and Δm.

3.2.1 The oblique parameter T

To conclude with the radiative corrections of the electroweak parameters within this model, constraints coming from the oblique parameter T will be consider here.

In Section 3.1, the parameter space of the model was derived using arguments of unitarity, BFB and the absence of tachyonic modes. It was evident from Figure 3.1 that the allowed region for the mass hierarchy $m_{\delta^{++}} > m_{H^+} > m_\theta$ was larger than the one for the inverse mass hierarchy, although both configurations were possible. Nevertheless, this "preference" disappears once the constraints derived from the electroweak oblique parameter T are considered. For an upper value of $v_\delta \sim 1$ GeV, the major contribution to the T-parameter comes from the loops involving the new triplet-like scalars. In this limit, $s_\alpha \approx 0$ and $m_H \approx m_\theta$, the new physics contribution to the electroweak T-parameter is given by [21]

$$\Delta T = \frac{1}{4\pi s_W^2 m_W^2}\left[F(m_{H^+}^2, m_\theta^2) + F(m_{\delta^{++}}^2, m_{H^+}^2)\right] , \tag{3.17}$$

where

$$F(x,y) = \frac{x+y}{2} - \frac{xy}{x-y}\ln\left(\frac{x}{y}\right) . \tag{3.18}$$

Equation (3.17) can be simplified from (2.38) and (3.18) in such a way that it depends only on the quantity $\Delta m = \Delta m_{\delta H^+} \approx \Delta m_{H^+\theta}$ [21]:

$$\Delta T \approx \frac{\Delta m^2}{3\pi s_W^2 m_W^2} . \tag{3.19}$$

Being the current experimental limit on the T-parameter of $\Delta T < 0.2$ with a 95% C.L. [18], it translates into an upper limit for the mass splitting of $|\Delta m| \lesssim 50$ GeV.

In Figure 3.10 (left) the allowed values for $\Delta m_{\delta H^+}$ computed in Section 3.1 are shown alongside

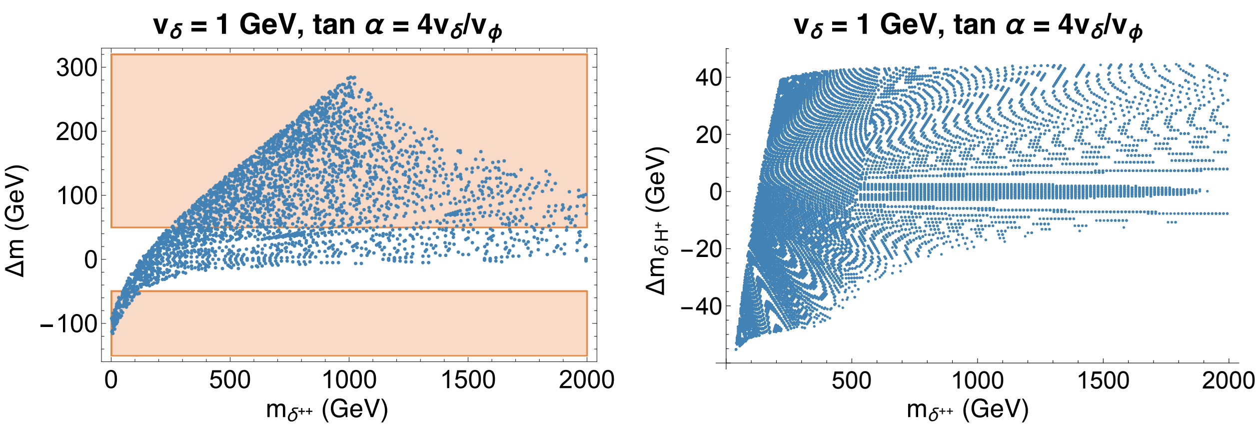

Figure 3.10: *For the left figure, in blue, the results from the computation of the mass difference $\Delta m_{\delta H^+}$ using arguments of unitarity, vacuum stability and the absence of tachyonic modes. In orange, the allowed region for the mass difference Δm from the EW oblique parameter T. The right figure shows the allowed values for $\Delta m_{\delta H^+}$ after the constraints from the corrections of the oblique T parameter were considered.*

with the constraints coming from the T parameter. Figure 3.10 (right) shows the allowed values for $\Delta m_{\delta H^+}$ after imposing the T correction, for this Figure a more exhaustive scan was performed within the allowed region.

3.3 Light Higgs decay into photons

Being the Higgs the lightest of the scalar particles of the model, there is not any decay channel for the Higgs particle to be tested at tree level for this model. Going to higher levels in a perturbative expansion, the most important difference should appear at the $h \to \gamma\gamma$ channel, as the photon is a massless particle and therefore does not couple to the Higgs at tree level, its first contribution to the $h\gamma\gamma$ vertex appears at the one-loop level. Now that two new charged particles (H^+ and δ^{++}) have been introduced, new contributions will appear and therefore the decay width $\Gamma(h \to \gamma\gamma)$ could vary notably from the SM prediction.

It can be noted that the production of this particle at the LHC does not vary in a first approximation. Being the main production mechanisms gluon fusion, VBF, and associated productions with VB and top quarks, as the new particles do not couple to gluons (do not have colour charge) or quarks (it is not possible to build up a singlet of hypercharge involving the quark doublets and the Higgs triplet for the Lagrangian).[1] Therefore, the production cross sections should not differ notably from the one predicted by the SM. Even though, the modified Higgs production cross section and total decay width can be redefined (as a ratio compared to the SM value) as follows:

$$\mathcal{R}_{\text{CS}} = \frac{\sigma(pp \to h)}{\sigma_{\text{SM}}(pp \to h)} = \kappa_F^2 (f_{ggF} + f_{t\bar{t}H}) + \kappa_W^2 (f_{\text{VBF}} + f_{\text{V}h}), \tag{3.20}$$

$$\mathcal{R}_{\text{TDW}} = \frac{\Gamma}{\Gamma_{\text{SM}}} = 0.76\, \kappa_F^2 + 0.24\, \kappa_W^2, \tag{3.21}$$

where 0.24 is the numerical value for BR$(h \to VV^*)$ and 0.76 is the approximate value of the branching ratio to other particles [18]. The f_X functions in (3.20) correspond to the percentage of the Higgs boson production through the X channel, being: $f_{ggF} \simeq 0.87$, $f_{t\bar{t}h} \simeq 5 \cdot 10^{-3}$, $f_{\text{VBF}} \simeq 0.07$ and $f_{\text{V}h} \simeq 0.05$ [18]. The κ_X functions are corrections to the SM cubic couplings of the Higgs with the field X, defined as:

$$\kappa_X \equiv \frac{\lambda_{hXX^*}}{\lambda_{hXX^*}^{\text{SM}}}. \tag{3.22}$$

The expression of the κ_X functions appearing in (3.20) and (3.21) are:

$$\kappa_F = c_\alpha, \qquad \kappa_V = s_\alpha s_\tau + c_\alpha c_\tau. \tag{3.23}$$

The decay width of $h \to \gamma\gamma$ has been computed at the one-loop level (see Appendix C), being for this model:

$$\Gamma(h \to \gamma\gamma) = \frac{G_F\, \alpha_{\text{em}}^2 m_h^3}{128\sqrt{2}\pi^3} \left| -2\kappa_q N_f^c q_f^2 \mathcal{F}_{1/2}(f) + \kappa_W \mathcal{F}_1(W) + q_j^2 \lambda_{j^*jh} \frac{v}{2m_j^2} \mathcal{F}_0(j) \right|^2, \tag{3.24}$$

where the first two terms correspond to the SM decay width for $\kappa_q = \kappa_W = 1$.

[1]In the limit of $\alpha \to 0$, where the triplet and doublet particle do not mix up to tiny corrections.

The $\mathcal{F}_i(x)$ functions are defined as in [27]:

$$\begin{aligned}\mathcal{F}_{1/2}(x) &= \tau_x[1+(1-\tau_x)f(\tau_x)],\\ \mathcal{F}_1(x) &= 2+3\tau_x+3\tau_x(2-\tau_x)f(\tau_x),\\ \mathcal{F}_0(x) &= \tau_x[1-\tau_x f(\tau_x)],\end{aligned} \tag{3.25}$$

being $f(x)$ and τ_j:

$$f(x) = \begin{cases} \Big[\arcsin(1/\sqrt{x})\Big]^2, & \text{if } x \geq 1 \\ -\frac{1}{4}\Big[\log\dfrac{1+\sqrt{1-x}}{1-\sqrt{1-x}} - i\pi\Big]^2, & \text{if } x < 1 \end{cases}, \qquad \tau_j = 4m_j^2/m_h^2. \tag{3.26}$$

In Eq. (3.24), $q_{f,j}$ is the electric charge of the field f, j and N_f^c is the colour factor. The index f corresponds to the set of charged fermions, although for later computations only the top and bottom quarks will be relevant. The index j stands for the charged scalars H^+ and δ^{++}.

From Equations (3.1 - 3.6), the couplings $\lambda_{H^+H^-h}$ and $\lambda_{\delta^{++}\delta^{--}h}$ that appear in Equations (D.1) and (D.2) have been redefined in terms of the physical masses and the triplet-doublet mixing angles as follows:

$$\lambda_{H^+H^-h} = \frac{1}{v_\delta}\left[m_{H^+}^2\left(\sqrt{2}s_\beta c_\beta c_\alpha + 2s_\beta^2 s_\alpha\right) - m_\theta^2 s_\alpha\left(c_\tau^2 + \frac{s_\tau^2}{2}\right) + m_h^2\left(\frac{s_\beta^3 c_\alpha}{\sqrt{2}c_\beta} + c_\beta^2 s_\alpha\right)\right], \tag{3.27}$$

$$\lambda_{\delta^{++}\delta^{--}h} = \frac{1}{v_\delta}\left[2m_{\delta^{++}}^2 s_\alpha + m_h^2 s_\alpha - 2m_{H^+}^2\left(2c_\beta^2 s_\alpha - \sqrt{2}s_\beta c_\beta c_\alpha\right) - m_\theta^2\left(s_\tau c_\tau c_\alpha - c_\tau^2 s_\alpha\right)\right]. \tag{3.28}$$

The decay rate $R_{\gamma\gamma}$ is then given as:

$$R_{\gamma\gamma} = \frac{\Gamma(h\to\gamma\gamma)}{\Gamma_{\text{SM}}(h\to\gamma\gamma)} = \frac{\left|-2N_f^c q_f^2 \mathcal{F}_{1/2}(f) + \mathcal{F}_1(W) + q_j^2 \lambda_{j^*jh}\frac{v}{2m_j^2}\mathcal{F}_0(j)\right|^2}{\left|-2N_f^c q_f^2 \mathcal{F}_{1/2}(f) + \mathcal{F}_1(W)\right|^2}, \tag{3.29}$$

and finally, the signal strength is defined as:

$$\mu_{\gamma\gamma} = \frac{\sigma\cdot\text{BR}^{\gamma\gamma}}{(\sigma\cdot\text{BR}^{\gamma\gamma})_{\text{SM}}} = \frac{\mathcal{R}_{\text{CS}}}{\mathcal{R}_{\text{TDW}}}\mathcal{R}_{\gamma\gamma}. \tag{3.30}$$

This signal strength has been computed for the complete parameter space allowed by the vacuum stability, unitarity and absence of tachyonic modes conditions and imposing the constraints of the T parameter, i.e. using the parameter space computed in Section 3.2.1. The result is shown in Figure 3.11 (left) as a function of the doubly charged scalar for the input value of $v_\delta = 1$ GeV. The green region correspond to the 2σ allowed space, from the experimental value $\mu_{\gamma\gamma}^{\text{exp}} = 1.16 \pm 0.18$ [18]. It can be seen in the figure that if the experimental error decreases and the experimental value remains around 1.15, then the value of the doubly charged scalar would have an upper bound on ~ 500 GeV. On the other hand, if the data starts to favour a value of $\mu_{\gamma\gamma}$ around unity, then the constraint for the doubly charged mass would disappear, as all values for $m_{\delta^{++}}$ would be allowed from this constraint.

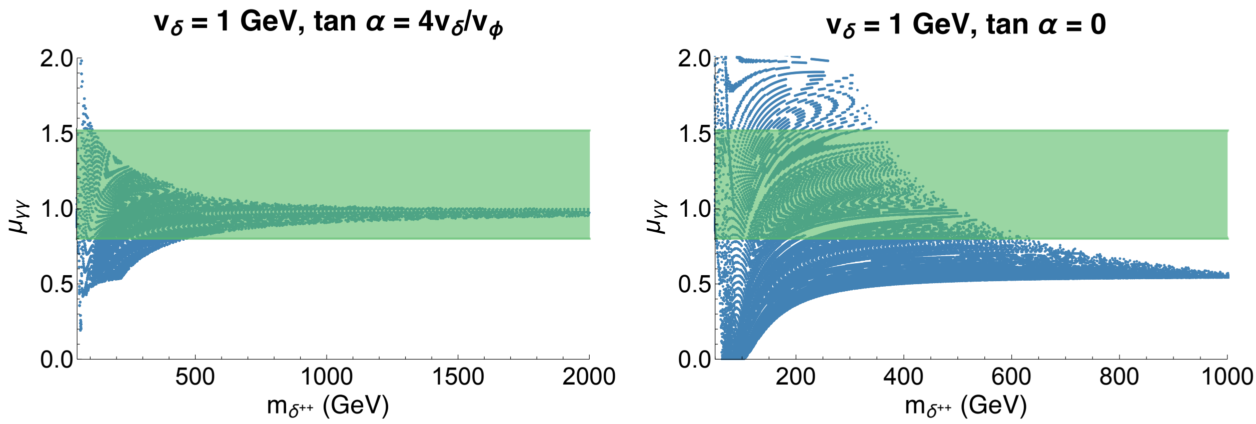

Figure 3.11: *In the left figure, the allowed values for the signal strength for the process $h \to \gamma\gamma$ predicted by the HTM as a function of $m_{\delta^{++}}$ for $\tan\alpha = 4v_\delta/v_\phi$ are shown. In the right figure the results of the same computation appear, now setting $\tan\alpha = s_\alpha = 0$. For both figures, the values $m_h = 125$ GeV, $m_t = 173$ GeV and $m_b = 4.7$ GeV have been used. The green region correspond to the 2σ allowed space, from the experimental value $\mu^{exp}_{\gamma\gamma} = 1.16 \pm 0.18$ [18]. The left figure has been computed using nothing else but the arguments of unitarity, vacuum stability, the absence of tachyonic modes and the constraints coming from the oblique parameter T. For the right Figure the constraints coming from the oblique parameter T have been omitted.*

The computation has been done considering values of $m_{\delta^{++}}$ from 1 GeV up to 2 TeV.

In the naive decoupling limit, i.e. $s_\alpha \to 0$ the contribution of the triplet-like particles is destructive with respect to the SM one. In fact, it can be easily checked from (3.28) that:

$$\lambda_{H^+H^-h} = \frac{1}{v_\delta}\left[m^2_{H^+}\sqrt{2}s_\beta c_\beta + m_h^2\frac{s_\beta^3}{\sqrt{2}c_\beta}\right] \simeq \frac{2m^2_{H^+}}{v}, \tag{3.31}$$

$$\lambda_{\delta^{++}\delta^{--}h} = \frac{1}{v_\delta}\left[2m^2_{H^+}\sqrt{2}s_\beta c_\beta - m_\theta^2 s_\tau c_\tau\right] \simeq \frac{2}{v}\left[2m^2_{H^+} - m^2_\theta\right] \simeq \frac{2m^2_{\delta^{++}}}{v}. \tag{3.32}$$

Taking the limit m_{charged} to be large, $\mathcal{F}_0(m_{\text{charged}})$ goes to $-1/3$. Therefore, the signal strength would be smaller than unity and would lie around $0.5 - 0.6$ in the $s_\alpha = 0$ case, as shown in Figure 3.11 (right), where the constraints coming from the oblique parameter T have been omitted for the computation in this limit. This configuration is therefore excluded, for any value of v_δ. If the value of s_α is relaxed, then terms from (3.28) that did vanished in that limit lead to a decoupling behaviour for large values of m_{charged}, as shown in Figure 3.11 (right). The fact that this strong variation appears when one sets s_α to be zero (right) compared to the limit of $s_\alpha = 2v_\delta/v_\phi \sim 0.008$ (left) is due to dependence of the couplings $\lambda_{H^+H^-h}$ and $\lambda_{\delta^{++}\delta^{--}h}$ on these small variations. Contrary to what happened with the couplings of the scalar particles with gauge bosons in Section 3.2, where the limit s_α was taken, the trilinear couplings between scalar particles are highly sensitive to small variations of their input parameters.

3.4 Triplet-like particle decays

Another important feature of the HTM is the introduction of a doubly-charged scalar, in addition to the singly-charged and the neutral scalars. This particle content would have consequences in the leptonic and gauge sectors that could play an important role for testing this model at the LHC. The study of the decay channels of the doubly-charged scalar will be the main goal of this Section. Nonetheless, a brief comment will be done for the neutral and singly charged scalar decays as well.

3.4.1 Neutral scalars decay

Although one expects the main decay channels for these particles, being triplet-like, to be into neutrinos, one can realise from the fact that the coupling depends on the particle masses, that the branching ratio into this decay channel will be notably smaller than the ones coming from its doublet-like component. In fact, by a simple computation and expecting $m^{(\nu)} \sim$ eV, one gets:

$$\frac{\text{BR}(X \to \bar{\nu}\nu)}{\text{BR}(X \to \bar{\ell}\ell)} \sim 10^{-5}, \tag{3.33}$$

where X stands for H and θ.

For the neutral scalar, H, using the same data for the BR as in Section 3.3, as now the leptonic and jet decays will have a redefinition of the vertex by a factor of s_α for the decay of $H \to \bar{\ell}\ell$ (or quarks), the branching ratio for the decay into gauge bosons will be larger than the leptonic or quark decay, for the expected value of $v_\delta < 10$ GeV.

In the case of the pseudoscalar, θ, its main decay channel would be the one into a gauge boson plus a scalar, as the ratio of the branching ratio has been computed, being:

$$\frac{\text{BR}(\theta \to hZ)}{\text{BR}(\theta \to \bar{\ell}\ell)} \sim \frac{m_\theta^2}{m_\ell^2}, \tag{3.34}$$

where all the masses except for the θ particle have been neglected (this can be done by assuming $m_\theta \sim 500$ GeV $> m_t$). The computation has been performed with h as a simplification, as the other scalars of the theory could be heavier than θ.

3.4.2 Charged scalar decay

In this case, the decay $H^+ \to \ell^+\nu$ is again suppressed by the coupling being proportional to the neutrino masses. Therefore, and following the same reasoning as for the neutral scalars, the decay into gauge bosons and into leptons or quarks via its doublet component has been analysed. This has been done in [28], where the following relation is obtained:

$$\frac{\text{BR}(H^+ \to t\bar{b})}{\text{BR}(H^+ \to W^+Z)} \sim 6\left(\frac{m_t}{m_{H^+}}\right)^2, \tag{3.35}$$

which means that for $m_{H^+} \gtrsim 500$ GeV, the decay into gauge bosons will dominate. The decay mode $H^+ \to t\bar{b}$ appears as it is the important decay channel coming from the doublet component of the H^+ field.

It is evident that, being the main decays of H^+ and H those coming from its doublet component, no dependence of the triplet vev, v_δ, appear on their branching rations.

3.4.3 Doubly charged scalar decay

The doubly charged scalar will leave recognisable imprints when produced at LHC. Therefore, it would be interesting to know which would be the main decay channels for this particle, and how those decay widths depend on the measurable quantities of the model like the masses or the vev, v_δ. Once those quantities are measured, the triplet-like behaviour of the δ^{++} particle could be tested. The decay widths for the different channels have been computed.

Leptonic decays

The δ^{++} decay into same-sign charged leptons is an interesting way to probe the neutrino masses and mixings, once the parameters $m_{\delta^{++}}$ and v_δ are determined. The decay width has been computed and its expression is the following:

$$\Gamma(\delta^{++} \to \ell_i^+ \ell_j^+) = \frac{m_{\delta^{++}}}{8\pi(1+\delta_{ij})} \left| \frac{(M_\nu)_{ij}}{v_\delta} \right|^2 . \tag{3.36}$$

Gauge boson decays

For the decay channel into gauge bosons the neutrino masses do not appear as unknown variables in the decay width expression, being:

$$\Gamma(\delta^{++} \to W^+W^+) = \frac{g^4}{16\pi} \frac{v_\delta^2}{m_{\delta^{++}}} \sqrt{1 - \frac{4m_W^2}{m_{\delta^{++}}^2}} \left[2 + \left(\frac{m_{\delta^{++}}^2}{2m_W^2} - 1 \right)^2 \right], \tag{3.37}$$

therefore, allowing to fix the value of v_δ from $m_{\delta^{++}}$. In the limit of large values of $m_{\delta^{++}}$ the following aproximation is obtained:

$$\Gamma(\delta^{++} \to W^+W^+) \approx \frac{g^4}{16\pi} \frac{v_\delta^2}{m_{\delta^{++}}} \left(\frac{m_{\delta^{++}}^2}{2m_W^2} \right)^2 = \frac{v_\delta^2}{4\pi v^4} m_{\delta^{++}}^3 . \tag{3.38}$$

Therefore, comparing (3.36) and (3.38):

$$\frac{\mathrm{BR}(\delta^{++} \to \ell^+\ell^+)}{\mathrm{BR}(\delta^{++} \to W^+W^+)} \simeq 2 \left(\frac{v}{v_\delta} \right)^4 \left(\frac{m_\nu}{m_{\delta^{++}}} \right)^2 . \tag{3.39}$$

Cascade decay

Another possibility would be, if the masses of the triplet-like particles are non-degenerated, what is known as cascade decay, i.e. the possibility of $\delta^{++} \to H^+\ell^+\nu$ via a virtual W^+ or $\delta^{++} \to H^+W^{+*} \to HW^{+*}W^{+*}$. Using the expressions for $\delta^{++} \to H^+\ell^+\nu$ and $\delta^{++} \to H^+q\bar{q}'$ from [28]:

$$\Gamma(\delta^{++} \to H^+\ell^+\nu) = \frac{\Delta m_{\delta H^+}^5}{60\pi^3 v^4}, \tag{3.40}$$

$$\Gamma(\delta^{++} \to H^+q\bar{q}') = 3\Gamma(\delta^{++} \to H^+\ell^+\nu). \tag{3.41}$$

The decay widths can be computed for the three most important decay channels for δ^{++}. Thus, the decay width for the processes $\delta^{++} \to H^+X$, X being $\ell^+\nu$ or $q\bar{q}'$ is:

$$\Gamma(\delta^{++} \to H^+X) = \frac{3}{20} \frac{\Delta m_{\delta H^+}^5}{\pi^3 v^4}, \tag{3.42}$$

where the decay mode $\delta^{++} \to H^+t\bar{b}$ has not been considered for the computation of Figure 3.12 for simplicity.[2] For the computation of the result shown in (3.42), a summation over all the possible

[2] The consideration of the decay mode $\delta^{++} \to H^+t\bar{b}$ will introduce a factor $(4/3)^{1/5} \sim 1.06$ of increase to the Δm boundary of the leptonic decay, and thus have been neglected.

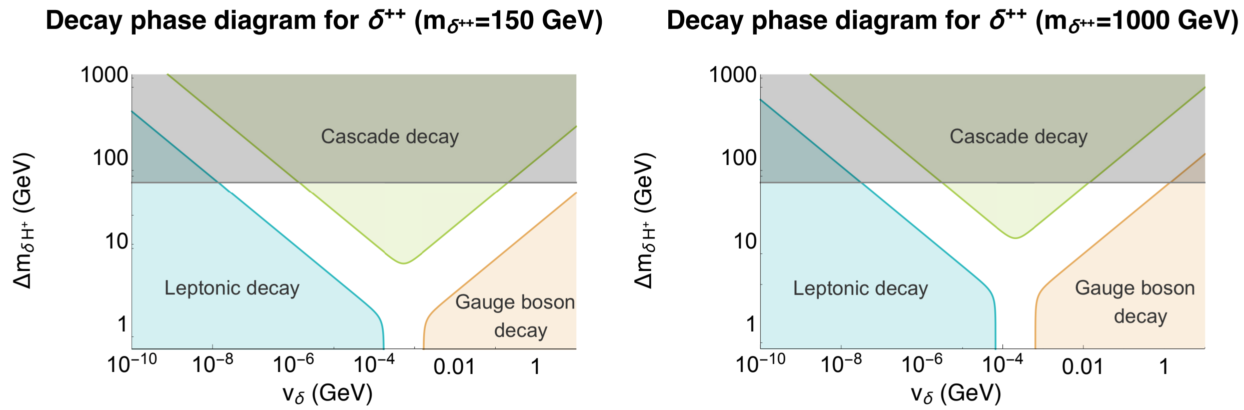

Figure 3.12: *Decay phase diagram for the δ^{++} particle decays in the HTM. For this Figure the mass $m_{\delta^{++}}$ has been fixed to 150 GeV (left) and 1000 GeV (right). The solid contour correspond to 99% of the branching ratio for the corresponding decay channel. $\Delta m_{\delta H^+}$ has been defined to be as in the text, $\Delta m_{\delta H^+} = m_{\delta^{++}} - m_{H^+}$. The grey region correspond to the excluded values of $\Delta m_{\delta H^+}$ from the T parameter.*

fermionic channels was done.

Similarly to what was done in [29], where $m_{\delta^{++}}$ has been fixed to be 150 GeV, the decay phase diagram has been computed here for two different values of $m_{\delta^{++}}$, in order to see how differences appear. The results are shown in Figure 3.12 for the values of $m_{\delta^{++}}$ to be 150 GeV (left) and 1 TeV (right). The boundary correspond to the value of BR$(\delta^{++} \to X)$ being 0.99. It is evident that there are no important differences appearing between the $m_{\delta^{++}} = 150$ GeV and $m_{\delta^{++}} = 1$ TeV cases.

The constraints coming from the T parameter imply that the main decay channels would correspond to leptons for $v_\delta < 10^{-4}$ GeV and gauge bosons for $v_\delta > 10^{-3}$ GeV. The cascade decay for the δ^{++} particle will be the preferred decay channel for the small region of $v_\delta \sim 10^{-3} - 10^{-4}$ GeV and for $\Delta m_{\delta H^+} > 10$ GeV.

4 Current LHC constraints on new scalars

4.1 Scalar searches at LHC

The enlargement of the scalar sector proposed by the HTM opens the possibility of a whole new rich phenomenology. Finding signs of new physics such as the scalars the HTM introduces is one of the goals of the LHC and the ATLAS and CMS collaborations. In this Chapter the searches at LHC of the neutral, singly charged and doubly charged are briefly commented, where the most important constraint is obtained for the doubly charged scalar, as this particle would leave the most recognisable imprints on the detector in this model. An brief comment on the κ parameters will be done in Section 4.2.

4.1.1 Neutral scalar

Searches for BSM particles are performed by the CMS and ATLAS collaborations. Their main focus have been the $Z\gamma$ and $\gamma\gamma$ resonances when it refers to the search for neutral scalar particles [30, 31].

An analysis based on a sample of pp collisions collected by the CMS experiment in 2016 at $\sqrt{s} = 13$ TeV, corresponding to an integrated luminosity of 12.9 fb^{-1} was performed in [30]. No significant excess was observed above the predictions of the standard model for these channels, where masses from 0.5 TeV up to 4.5 TeV were explored. For $m = 750$ GeV, the excess with 3.4 standard deviation local significance once measured by [32] has been reduced to about 1.9 standard deviations.

In [31], a search for spin-0 $Z\gamma$ resonances in the hadronic decay channel of the Z boson, combined with some previously published results of the search in the leptonic decay channels [33] was performed. The combination and analysis is based on data sets recorded with the CMS detector at the LHC in pp collisions at CM energies of 8 and 13 TeV, corresponding to integrated luminosities of 19.7 fb^{-1} and 2.7 fb^{-1}, respectively. The search was performed in the mass range from 0.65 to 3.0 TeV. Again, no significant deviation from the standard model prediction is found. For this study it was assumed that the mechanism for production of a new resonance is gluon fusion, as happens to be for this model.

4.1.2 Charged scalar

The search of a charged Higgs, H^+ has been performed at the LHC for both collaborations, ATLAS and CMS, using data from the two runs. Different possibilities for the charged scalar have been studied as its decay into τ+jets [34], jets [35], $\tau^+\nu$ [36] and gauge bosons [37] have been explored. Those channels have been tested and no discrepancies with respect to the SM have been measured [36, 37]. These analyses set an upper limit in the cross section of the different processes. Being the SM background large enough, the different masses have not been excluded, but a limit is set on the cross section for the different mass values. The data collected from the CMS collaboration and the subsequent analysis extend up to 3 TeV.

In [37], the process $pp \to H^+ \to W^+ Z$ via VBF has been analysed at energies of $\sqrt{s} = 13$ TeV. The data sample corresponds to an integrated luminosity of 15.2 fb^{-1}. The associated Feynman diagram for the LO contribution to the VBF generation of H^+ decaying into vector bosons is shown in Figure 4.1.

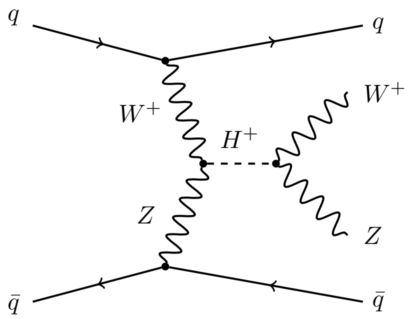

Figure 4.1: *Associated Feynman diagram for the $pp \to H^+ \to W^+ Z$ process at LO.*

A combined fit of the data was performed to derive expected and observed exclusion limits on $\sigma_{\text{VBF}}(H^\pm) \cdot \text{BR}(H^\pm \to W^\pm Z)$ at 95% CL. The exclusion limits as a function of $m_{H^\pm}$ are shown in Figure 4.2. Values for $\sigma_{\text{VBF}}(H^\pm) \cdot \text{BR}(H^\pm \to W^\pm Z)$ from 573 fb at $m_{H^\pm} = 200$ GeV to 36 fb at $m_{H^\pm} = 2000$ GeV are excluded by the data.

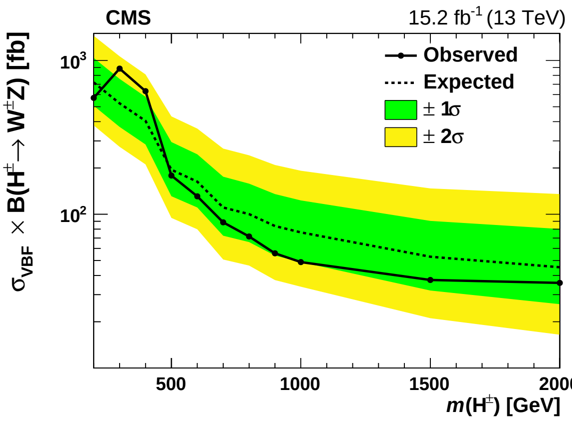

Figure 4.2: *Expected and observed exclusion limits at 95% confidence level for $\sigma_{VBF}(H^\pm) \cdot BR(H^\pm \to W^\pm Z)$ as a function of m_{H^+} for $15.2\,fb^{-1}$ of pp collisions at $\sqrt{s} = 13$ TeV collected in 2015 and 2016.*

In [38], the quantity $\sigma_{\text{VBF}}(H^\pm)$ has been computed using an input value of the form factor[1] $F = 1$. Here, using the results in [38], $\sigma_{\text{VBF}}(H^\pm) \cdot \text{BR}(H^\pm \to W^\pm Z)$ for the HTM has been estimated. From [38, 39] and the coupling from Appendix D, the form factor has been computed for the HTM, being:

$$F^{\text{HTM}} = \frac{2 s_\beta c_\beta}{c_W}, \tag{4.1}$$

[1]The form factor F is the coefficient of the $g_{\mu\nu}$ term contribution to the $H^\pm W^\mp Z$ vertex, being the most important contribution to $\sigma_{\text{VBF}}(H^\pm)$, [38].

that goes from 10^{-6} up to 10^{-2} for $v_\delta = 0.1$ GeV and 10 GeV respectively, i.e.:

$$\frac{\sigma_{\text{VBF}}(H^\pm)\cdot \text{BR}(H^\pm \to W^\pm Z)|_{F^{\text{HTM}}}}{\sigma_{\text{VBF}}(H^\pm)\cdot \text{BR}(H^\pm \to W^\pm Z)|_{F=1}} \sim 10^{-12} - 10^{-4}. \tag{4.2}$$

Doing the computations with the input $\sigma_{\text{VBF}}(H^\pm)\cdot \text{BR}(H^\pm \to W^\pm Z)|_{F=1}$, the following results are obtained:

$$\sigma_{\text{VBF}}(H^\pm)\cdot \text{BR}(H^\pm \to W^\pm Z)|_{\text{HTM},\, m_{H^\pm}=200\text{ GeV}} \lesssim 0.25\text{ fb}, \tag{4.3}$$

$$\sigma_{\text{VBF}}(H^\pm)\cdot \text{BR}(H^\pm \to W^\pm Z)|_{\text{HTM},\, m_{H^\pm}=2000\text{ GeV}} \lesssim 5\cdot 10^{-4}\text{ fb}, \tag{4.4}$$

It is evident that the constraints on the cross section for the charged scalar do not impose any meaningful constraint for the HTM, as the upper limit for the cross section for masses going from 200 GeV up to 2000 GeV are orders of magnitude higher than the expected for this model.

4.1.3 Doubly charged scalar

Searches for the doubly-charged Higgs boson in pp collisions at $\sqrt{s} = 13$ TeV with the CMS experiment at the LHC have been performed [40]. The search, whose associated Feynman diagrams are shown in Figure 4.3, considers final states with four (left) and three (right) lepton final states coming from the associated production via $q\bar{q} \to Z/\gamma \to \delta^{\pm\pm}\delta^{\mp\mp} \to \ell^+\ell^+\ell^-\ell^-$ and $qq' \to W^\pm \to \delta^{\pm\pm}H^\mp \to \ell^+\ell^+\ell^-\nu$ respectively. Since the branching fractions are not fixed by the model, the analysis performed by the CMS collaboration is model independent, although BR($\delta^{++} \to$ *leptons*) has been set to be 100%.

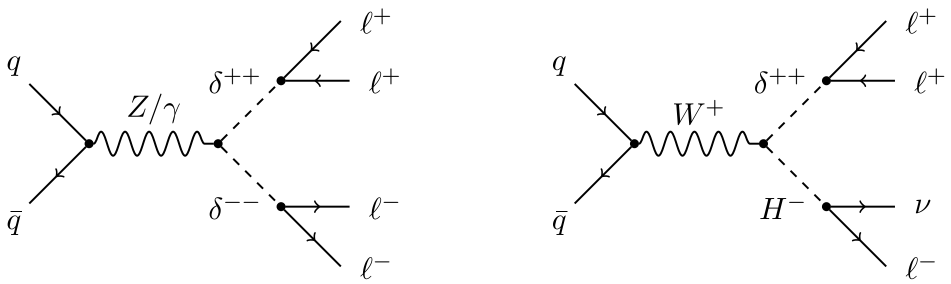

Figure 4.3: *Feynman diagrams associated to the four (left) and three (right) lepton channels explored by the CMS collaboration.*

Lower bounds on the doubly-charged Higgs boson mass have been derived for a variety of assumptions on its branching ratio to charged lepton pairs and on the neutrino mass configurations, as no significant excess over the SM background has been observed for any of these assumptions. The actual lower bounds on the δ^{++} mass for the type II see-saw model lies between $\sim 715 - 760$ GeV with a 95% CL [40] for δ^{++} decaying into leptonic final states, i.e. for $v_\delta < 10^{-4}$ GeV (see Figure 3.12). For this analysis a sample of 12.9 fb^{-1} of integrated luminosity from 2016 was used.

4.2 The κ_X parameters

A modification of the scalar sector with respect to the SM implies some changes on the couplings of the Higgs particle with all the particles from the SM, as was seen in Section 2.5 for the leptonic sector. This modification can be parametrised using the kappa approach, valid for any BSM model. If the couplings of different particles are measured with enough precision and those differ from unity, it should be analysed as it could be the sign of new physics.

For the computation of the signal strength $\mu_{\gamma\gamma}$ in Section 3.3, the parameters κ_X were defined:

$$\kappa_X \equiv \frac{\lambda_{hXX}}{\lambda_{hXX}^{\text{SM}}}. \tag{4.5}$$

These relative coupling parameters have been measured at LHC and the data on the triplet vev should be considered alongside with the constraints studied on previous sections. From [18], the combined measurements of these parameters for the gauge bosons and fermions are:

$$\kappa_V^{\text{exp}} = 1.04 \pm 0.05, \qquad \kappa_F^{\text{exp}} = 0.98^{+0.11}_{-0.10} \tag{4.6}$$

From the couplings in Appendix D, the constraints on v_δ can be obtained, as:

$$\kappa_F = c_\alpha, \qquad \kappa_V = s_\alpha s_\tau + c_\alpha c_\tau. \tag{4.7}$$

These constraints have been computed for different values of v_δ and they are contained within the allowed region for values up to $v_\delta \sim 100$ GeV. Thus, the constraints coming from the κ parameters are much softer than the ones imposed by the ρ parameter.

5 Discussion

There are strong evidences supporting the need of physics beyond the SM. Here a possible extension of the scalar sector by a $SU(2)_L$ triplet with hypercharge $y_\delta = 2$ has been studied, being particularly interesting as it is able to explain the smallness of neutrino masses because of the type II seesaw mechanism.

In Chapter 2 the model was introduced, the masses of the new scalar particles were obtained and some theoretical constrains were discussed. Later, a brief discussion about the seesaw type II mechanism was done and some consequences in the leptonic sector were commented.

Phenomenological implications of the model were explored in Chapter 3. First, the allowed parameter space of the HTM was derived using a fixed value for the triplet vev, $v_\delta = 1$ GeV. The computations were repeated with v_δ to be 5 GeV and 10 GeV and no significant differences appeared. From the allowed parameter space of the model and the experimental limits on the oblique parameter T, the masses of the model are restricted to be almost degenerate, as the mass differences $m_{\delta^{++}} - m_{H^+} \approx m_{H^+} - m_\theta$ must not exceed the value of 50 GeV. Later, the study done in [7] on the model from the radiative corrections to m_W and ρ was introduced. These constraints would strongly favour the mass hierarchy of the model to be $m_{\delta^{++}} < m_{H^+} < m_\theta$, where a better agreement seems to be expected for $m_{\delta^{++}} < 150$ GeV by looking at Figures 3.4 and 3.6, and v_δ to be localised around $1 - 10$ GeV (for $m_{\delta^{++}} = 150$ GeV). Additionally, it was clear from Figures 3.6-3.9 that the experimental data would clearly disfavour θ being the lightest of the considered particles. Nevertheless, these results were obtained by supposing the same mass splitting between the three heavy particles, i.e. $m_{\delta^{++}} - m_{H^+} = m_{H^+} - m_\theta$. Therefore, the other mass hierarchy, $m_{\delta^{++}} > m_{H^+} > m_\theta$, should not be considered to be excluded, as the whole parameter space was not tested in [7].

Additionally, the diphoton channel of the Higgs boson was computed and the decoupling limit observed. The experimental value for the signal strength $\mu_{\gamma\gamma}$ did not set constraints on the masses of the particles as the predicted values are mostly contained inside the experimentally allowed region. There, the decoupling limit was checked and the limit of $s_\alpha = 0$ was excluded.

Last, the most important decay modes for the heavy particles of the model were obtained in Section 3.4 and in Chapter 4 the current LHC searches carried by the ATLAS and CMS collaborations for scalars were discussed. The main difficulties for both the direct and indirect searches for the scalars of the model are caused by the fact that they are mostly triplet-like particles and therefore their mixings with the SM particles are suppressed. This was clearly seen in Section 4.1.2, where the current limits on the cross section for the singly-charged scalar is of orders of magnitude higher than the expected theoretical value.

Acknowledgements

First of all, I would like to thank Toni for being such an excellent supervisor, for all the discussion we had during the development of this project and for always finding a place on his schedule.

I would like as well to express my gratitude to Arcadi Santamaría for being like a second advisor and for all the clarifying discussions we had along the year.

I would like to thank all the people of the MSc in Advanced physics with whom I have shared this year as well as Ana, Victor and Mario for the conversations and the back and forths.

Finally, I want to thank my parents and my brother, as without their support I would not have been able to pursue this master.

Appendix

A Conversion between different notations

Following the example of [19], a table for conversion between different notations for the parameters in the scalar potential and the doublet-triplet mixing angles is given.

Source	m_Φ^2	M^2	μ	λ	λ_1	λ_2	λ_3	λ_4	α	β	τ
[7]	m^2	M^2	μ	$4\lambda_1$	λ_4	λ_2	λ_3	λ_5	α	$\beta_\pm$	β_0
[19]	μ_H^2	μ_Δ^2	$\frac{1}{2}m_{H\Delta}$	$2\lambda_H$	$\lambda_{H\Delta}$	$\frac{1}{2}\lambda_\Delta$	$\frac{1}{2}\lambda'_\Delta$	$\lambda'_{H\Delta}$			
[20]	m_H^2	M_Δ^2	μ	λ	λ_1	λ_2	λ_3	λ_4	α	β'	β
[21]	m^2	M^2	μ	$4\lambda_1$	λ_4	λ_2	λ_3	λ_5	α	β	β'

Table 1: *Translation between the notation used in this paper and the one used by other authors.*

B The R_ξ-gauge

It is known that every spontaneously broken non-Abelian gauge theory contains Goldstone bosons. However, these Goldstone bosons are artefacts of the theory, this will be explicit once their propagators are presented, and therefore can be gauged away [41]. If the terms in Eq. (2.1) are expanded it could be found that, before introducing any gauge fixing term, this Lagrangian contains quadratic terms mixing gauge bosons and Goldstone bosons:

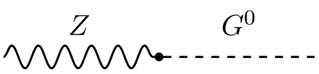

$$m_Z \, p^\mu_{G^0} \, , \tag{B.1}$$

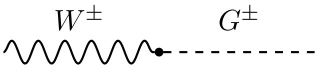

$$\mp \, i \, m_W \, p^\mu_{G^\pm} \, . \tag{B.2}$$

Nevertheless, these terms will disappear once the corresponding gauge transformation is performed.

Some particular gauges that are very useful in spontaneously-broken gauge theories are the R_ξ-gauges, where R stands for renormalizable and ξ is the gauge parameter. For the Abelian case, the R_ξ-gauges are defined by the gauge-fixing condition [42]:

$$f\left(A^a_\mu,\ G^a\right) = \partial_\mu A^\mu_a + \xi\, m_a G^a = 0\,. \tag{B.3}$$

Then, the gauge fixing Lagrange density is introduced as:

$$\mathcal{L}_{\rm GF} = -\frac{1}{2\xi}\left[\partial_\mu A^\mu_a + \xi\, m_a G^a\right]^2. \tag{B.4}$$

Therefore, in an Abelian theory after introducing the gauge fixing term the Lagrangian density defined as $\mathcal{L} = \mathcal{L}_0 + \mathcal{L}_{\rm GF}$ will not contain quadratic terms mixing A^μ_a and G^a.

In a non-Abelian case, i.e. the case here, the expression for the R_ξ gauge fixing term gets more complicated. Even so, it can checked that this term corresponds to [42]

$$\mathcal{L}_{\rm GF} = -\frac{1}{2\xi}\left[\partial_\mu A^\mu_a + \xi\left(\phi^+ L_a v - v^+ L_a \phi\right)\right]^2, \tag{B.5}$$

where the following compact notation is being used:

$$\phi = \left(\phi^+,\ \phi^0,\ \Delta^{++},\ \Delta^+,\ \Delta^0\right)^T, \qquad A^\mu_a = \left(\overrightarrow{W}^\mu,\ B^\mu\right)^T, \tag{B.6}$$

$$v = \frac{1}{\sqrt{2}}\left(0,\ v_\phi,\ 0,\ 0,\ v_\delta\right)^T, \qquad L_a = i\, g_a T^a = i\,\left(g\overrightarrow{T}, g'\,Y\right)^T. \tag{B.7}$$

This gauge fixing term yields to a redefinition of the propagators:

(i) Scalar propagator:

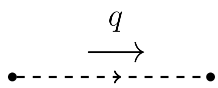

$$i\,\Delta_s(q) = \frac{i}{q^2 - m_s^2 + i\varepsilon}. \tag{B.8}$$

(ii) Goldstone boson propagator:

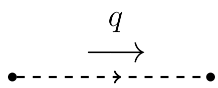

$$i\,\Delta_a(q) = \frac{i}{q^2 - \xi m_a^2 + i\varepsilon}. \tag{B.9}$$

It can be noted that the Goldstone bosons have acquired a squared-mass equal to ξm_a^2, i.e. a non physical mass. As stated before, this is understood as Goldstone bosons are artefacts of the gauge choice. The same will occur with the Faddeev-Popov ghosts.

(iii) Gauge boson propagator:

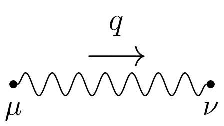

$$i\,\Delta_a^{\mu\nu}(q) = \frac{-i}{q^2 - m_a^2 + i\varepsilon}\left[g^{\mu\nu} - (1-\xi)\frac{q^\mu q^\nu}{q^2 - \xi m_a^2}\right]. \tag{B.10}$$

(iv) Ghost propagator:

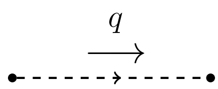

$$i\,\Delta_a(q) = \frac{i}{q^2 - \xi m_a^2 + i\varepsilon}. \tag{B.11}$$

Two useful gauges are $\xi = 1$ ('t Hooft-Feynman gauge) and $\xi = 0$ (Landau gauge), in which the Goldstone bosons are massless. Another interesting gauge, the unitary gauge, takes the limit of $\xi \to \infty$. In this gauge the Goldstone boson masses become infinite and thus decouple from all Feynman graphs, i.e. they disappear from the particle content of the theory.

C The Higgs to photons decay through charged scalars

In this appendix, the contribution of the charged scalars introduced by the HTM to the $h \to \gamma\gamma$ decay is derived. The diagrams corresponding to the charged scalar contributions are shown in Figure (C.1). Another diagram with two photon vertices but with the external photon lines crossed should be taken into account.

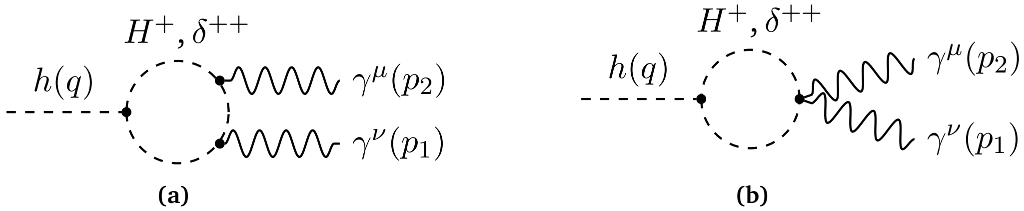

Figure C.1: *Contributions of the charged scalars H^+ and δ^{++} to the $h\gamma\gamma$ vertex. Another diagram with two photon vertices but with the photonic lines crossed should be considered.*

First, the computation of the contribution of the diagram (C.1a) is presented, using the corresponding Feynman rules from Appendix D. Here, λ_{jj^*h} represents the cubic coupling of the Higgs with the charged scalar j ($j = H^+$, δ^{++}) and e_j is the electric charge. The matrix element for the first diagram can be written as:

$$\mathcal{M}_{1\mathrm{a}} = \lambda_{jj^*h} e_i^2 \epsilon_2^\mu \epsilon_1^\nu \int \frac{d^D k}{(2\pi)^D} \frac{(2k+p_2)_\mu (2k-p_1)_\nu}{\left((k+p_2)^2 - m_j^2\right)\left((k-p_1)^2 - m_j^2\right)\left(k^2 - m_j^2\right)}. \tag{C.1}$$

As the photon is transversal, using that $\epsilon_i^\alpha p_{\alpha,i} = 0$ some terms cancel. Therefore:

$$\mathcal{M}_{1\mathrm{a}} = \lambda_{jj^*h} e_i^2 \epsilon_2^\mu \epsilon_1^\nu \int \frac{d^D k}{(2\pi)^D} \frac{4 k_\mu k_\nu}{\left((k+p_2)^2 - m_j^2\right)\left((k-p_1)^2 - m_j^2\right)\left(k^2 - m_j^2\right)}. \tag{C.2}$$

Now, using Feynman parametrization the integral can be rewritten as:

$$\int \frac{d^D k}{(2\pi)^D} \frac{k_\mu k_\nu}{\left((k+p_2)^2 - m_j^2\right)\left((k-p_1)^2 - m_j^2\right)\left(k^2 - m_j^2\right)} = \Gamma(3) \int_0^1 dx \int_0^1 dy\, x \int \frac{d^D k}{(2\pi)^D} \frac{k_\mu k_\nu + \eta_\mu \eta_\nu}{(k^2 - a^2)^3}, \tag{C.3}$$

where $\eta^\alpha \equiv p_1^\alpha x(1-y) - p_2^\alpha xy$ and $a^2 \equiv \eta^2 + m_j^2$. Using now:

$$\int \frac{d^D k}{(2\pi)^D} \frac{1}{(k^2 - a^2)^n} = \frac{(-1)^n i}{(4\pi)^{D/2}} \frac{\Gamma\left(n - \frac{D}{2}\right)}{\Gamma(n)} (a^2)^{D/2 - n}, \tag{C.4}$$

$$\int \frac{d^D k}{(2\pi)^D} \frac{k_\mu k_\nu}{(k^2-a^2)^n} = \frac{(-1)^{n-1} i}{(4\pi)^{D/2}} \frac{g_{\mu\nu}}{2} \frac{\Gamma\left(n-\frac{D}{2}-1\right)}{\Gamma(n)} (a^2)^{D/2-n+1}, \tag{C.5}$$

the following expression is obtained:

$$\Gamma(3) \int \frac{d^D k}{(2\pi)^D} \frac{k_\mu k_\nu}{(k^2-a^2)^3} = \frac{i}{2} \frac{g_{\mu\nu}}{(4\pi)^2} \Gamma(-\epsilon) \left(\frac{a^2}{4\pi}\right)^\epsilon = \frac{i}{2} \frac{g_{\mu\nu}}{(4\pi)^2} \left(-\frac{1}{\hat{\epsilon}} - \log\left(\frac{a^2}{4\pi}\right)\right), \tag{C.6}$$

$$\Gamma(3) \int \frac{d^D k}{(2\pi)^D} \frac{\eta_\mu \eta_\nu}{(k^2-a^2)^3} = -\frac{i}{(4\pi)^2} \frac{1}{a^2}, \tag{C.7}$$

where the term γ_E has been absorbed by a redefinition $1/\hat{\epsilon} \equiv 1/\epsilon + \gamma_E$, being ϵ defined as $\epsilon \equiv D-4$. Finally:

$$\mathcal{M}_{1\mathrm{a}} = 4 \frac{i}{(4\pi)^2} \lambda_{jj^*h} e_i^2 \epsilon_2^\mu \epsilon_1^\nu \int_0^1 dx \int_0^1 dy\, x \Big[\frac{g_{\mu\nu}}{2} \left(-\frac{1}{\hat{\epsilon}} - \log\left(\frac{a^2}{4\pi}\right)\right) - \frac{1}{a^2} \eta_\mu \eta_\nu \Big]. \tag{C.8}$$

It can be easily seen by doing an appropriate definition of the momenta that:

$$\mathcal{M}_{1\mathrm{a}} = \mathcal{M}_{2\mathrm{a}}. \tag{C.9}$$

Now, the matrix element for the diagram (C.1b) can be written as:

$$\mathcal{M}_{\mathrm{b}} = -2 \lambda_{jj^*h} e_i^2 \epsilon_2^\mu \epsilon_1^\nu g_{\mu\nu} \int \frac{d^D k}{(2\pi)^D} \frac{1}{\left((k+q)^2 - m_j^2\right)\left(k^2 - m_j^2\right)}. \tag{C.10}$$

Using Feynman parametrization:

$$\int \frac{d^D k}{(2\pi)^D} \frac{1}{\left((k+q)^2 - m_j^2\right)\left(k^2 - m_j^2\right)} = \Gamma(2) \int \frac{d^D k}{(2\pi)^D} \int_0^1 dx \frac{1}{(k^2-b^2)^2}, \tag{C.11}$$

where $b^2 \equiv q^2 x(x-1) + m_j^2$. Using (C.4):

$$\Gamma(2) \int \frac{d^D k}{(2\pi)^D} \int dx \frac{1}{(k^2-b^2)^2} = \frac{i}{(4\pi)^2} \int_0^1 dx \left(-\frac{1}{\hat{\epsilon}} - \log\left(\frac{b^2}{4\pi}\right)\right). \tag{C.12}$$

Therefore:

$$\mathcal{M}_{\mathrm{b}} = -2 \lambda_{jj^*h} e_i^2 \epsilon_2^\mu \epsilon_1^\nu g_{\mu\nu} \frac{i}{(4\pi)^2} \int_0^1 dx \left(-\frac{1}{\hat{\epsilon}} - \log\left(\frac{b^2}{4\pi}\right)\right). \tag{C.13}$$

Thus, the total matrix element is:

$$\begin{aligned} \mathcal{M} = 2\mathcal{M}_{1\mathrm{a}} + \mathcal{M}_{\mathrm{b}} = & \frac{2\, i}{(4\pi)^2} \lambda_{jj^*h} e_i^2 \epsilon_2^\mu \epsilon_1^\nu \Big[\int_0^1 dx \int_0^1 dy\, x \Big[2\, g_{\mu\nu} \left(-\frac{1}{\hat{\epsilon}} - \log\left(\frac{a^2}{4\pi}\right)\right) - \frac{4}{a^2} \eta_\mu \eta_\nu \Big] \\ & - g_{\mu\nu} \int_0^1 dx \left(-\frac{1}{\hat{\epsilon}} - \log\left(\frac{b^2}{4\pi}\right)\right) \Big], \end{aligned} \tag{C.14}$$

$$\begin{aligned}\mathcal{M} = \frac{2\,i}{(4\pi)^2}\lambda_{jj^*h}e_i^2\epsilon_2^\mu\epsilon_1^\nu\Bigg[g_{\mu\nu}\left(-2\int_0^1 dx\int_0^1 dy\, x\log\left(a^2\right)+\int_0^1 dx\log\left(b^2\right)\right)\\ -\int_0^1 dx\int_0^1 dy\, x\frac{4}{a^2}\eta_\mu\eta_\nu\Bigg],\end{aligned} \tag{C.15}$$

where both $\log(4\pi)^2$ canceled. Doing the x integral for $\log(a^2)$ and then the summation with the $\log(b^2)$ term:

$$-2\int_0^1 dx\int_0^1 dy\, x\log\left(a^2\right)+\int_0^1 dx\log\left(b^2\right)=\int_0^1 dy\left(1-\frac{m^2}{q^2(y-1)y}\log\left(\frac{q^2}{m^2}(y-1)y+1\right)\right). \tag{C.16}$$

In (C.16), the variable of integration x in the second integral has been renamed by y. Again, using the fact that the photon is transversal, the following expression is obtained for the last integral:

$$\int_0^1 dx\int_0^1 dy\, x\frac{4}{a^2}\eta_\mu\eta_\nu=\frac{p_{2,\mu}p_{1,\nu}}{p_1p_2}\int_0^1 dy\left(1-\frac{m^2}{q^2(y-1)y}\log\left(\frac{q^2}{m^2}(y-1)y+1\right)\right) \tag{C.17}$$

Therefore:

$$\mathcal{M}=\frac{2\,i}{(4\pi)^2}\lambda_{jj^*h}e_i^2\epsilon_2^\mu\epsilon_1^\nu\left(g_{\mu\nu}-\frac{p_{2,\mu}p_{1,\nu}}{p_1p_2}\right)\int_0^1 dy\left[1-\frac{m^2}{q^2(y-1)y}\log\left(\frac{q^2}{m^2}(y-1)y+1\right)\right] \tag{C.18}$$

Solving this integral for the cases where poles do and do not appear lead to the final expression:

$$\mathcal{M}=\frac{2\,i}{(4\pi)^2}\lambda_{jj^*h}e_i^2\epsilon_2^\mu\epsilon_1^\nu\left(g_{\mu\nu}-\frac{p_{2,\mu}p_{1,\nu}}{p_1p_2}\right)\Big[1-\tau_j f(\tau_j)\Big], \tag{C.19}$$

where

$$f(x)=\begin{cases}\Big[\arcsin(1/\sqrt{x})\Big]^2, & \text{if } x\geq 1,\\ -\dfrac{1}{4}\Big[\log\left(\dfrac{1+\sqrt{1-x}}{1-\sqrt{1-x}}\right)-i\pi\Big]^2, & \text{if } x<1,\end{cases}\qquad \tau_j=4m_j^2/m_h^2. \tag{C.20}$$

D Couplings

Cubic Higgs couplings

$$\begin{aligned}H^+H^-h = -\frac{i}{2}\Big[c_\alpha\left(v_\phi\left(2\lambda_1+\lambda_4\right)c_\beta^2+s_\beta\left(4\mu-\sqrt{2}v_\delta\lambda_4\right)c_\beta+\lambda s_\beta^2 v_\phi\right)\\ +\, s_\alpha\left(4v_\delta\left(\lambda_2+\lambda_3\right)c_\beta^2-\sqrt{2}s_\beta v_\phi\lambda_4 c_\beta+2s_\beta^2 v_\delta\lambda_1\right)\Big]\end{aligned} \tag{D.1}$$

$$\delta^{++}\delta^{--}h=-i(c_\alpha v_\phi\lambda_1+2s_\alpha v_\delta\lambda_2) \tag{D.2}$$

Cubic Higgs-gauge couplings

$$H^+H^-\gamma = ie\left(p_{H^-} - p_{H^+}\right)_\mu \tag{D.3}$$

$$\delta^{++}\delta^{--}\gamma = 2ie\left(p_{\delta^{--}} - p_{\delta^{++}}\right)_\mu \tag{D.4}$$

$$hW^+W^- = i\,g\,m_W\left(s_\alpha s_\tau + c_\alpha c_\tau\right)g_{\mu\nu} \tag{D.5}$$

$$hZZ = i\,2g\,m_Z\left(s_\alpha s_\tau + c_\alpha c_\tau\right)g_{\mu\nu} \tag{D.6}$$

$$H^+W^+Z = -i\,g\,\frac{m_W}{c_W}2s_\beta c_\beta g_{\mu\nu} \tag{D.7}$$

Quartic Higgs-gauge couplings

$$H^+H^-\gamma\gamma = 8ie^2 g_{\mu\nu} \tag{D.8}$$

$$\delta^{++}\delta^{--}\gamma\gamma = 2ie^2 g_{\mu\nu} \tag{D.9}$$

Bibliography

[1] CMS Collaboration, S. Chatrchyan *et al.*, "Observation of a new boson at a mass of 125 GeV with the CMS experiment at the LHC", *Phys. Lett.* B716 (2012) 30–61, arXiv:1207.7235 [hep-ex].

[2] CMS Collaboration, S. Chatrchyan *et al.*, "Observation of a new boson with mass near 125 GeV in pp collisions at $\sqrt{s} = 7$ and 8 TeV", *JHEP* 06 (2013) 081, arXiv:1303.4571 [hep-ex].

[3] ATLAS Collaboration, G. Aad *et al.*, "Observation of a new particle in the search for the Standard Model Higgs boson with the ATLAS detector at the LHC", *Phys. Lett.* B716 (2012) 1–29, arXiv:1207.7214 [hep-ex].

[4] ATLAS Collaboration, G. Aad *et al.*, "Measurements of Higgs boson production and couplings in diboson final states with the ATLAS detector at the LHC", *Phys. Lett.* B726 (2013) 88–119, arXiv:1307.1427 [hep-ex]. [Erratum: Phys. Lett.B734,406(2014)].

[5] J. Schechter and J. W. F. Valle, "Neutrino Masses in SU(2) x U(1) Theories", *Phys. Rev.* D22 (1980) 2227.

[6] M. Magg and C. Wetterich, "Neutrino Mass Problem and Gauge Hierarchy", *Phys. Lett.* B94 (1980) 61–64.

[7] S. Kanemura and K. Yagyu, "Radiative corrections to electroweak parameters in the higgs triplet model and implication with the recent higgs boson searches", *Physical Review D* 85 no. 11, (2012) 115009.

[8] G. Ria and D. Meloni, "Radiative corrections of heavy scalar decays to gauge bosons in the singlet extension of the Standard Model", arXiv:1705.11126 [hep-ph].

[9] K. Enqvist, S. Nurmi, T. Tenkanen, and K. Tuominen, "Standard Model with a real singlet scalar and inflation", *JCAP* 1408 (2014) 035, arXiv:1407.0659 [astro-ph.CO].

[10] G. C. Branco, P. M. Ferreira, L. Lavoura, M. N. Rebelo, M. Sher, and J. P. Silva, "Theory and phenomenology of two-Higgs-doublet models", *Phys. Rept.* 516 (2012) 1–102, arXiv:1106.0034 [hep-ph].

[11] P. Draper, H. E. Haber, and J. T. Ruderman, "Partially Natural Two Higgs Doublet Models", *JHEP* 06 (2016) 124, arXiv:1605.03237 [hep-ph].

[12] G. Bhattacharyya and D. Das, "Scalar sector of two-Higgs-doublet models: A minireview", *Pramana* 87 no. 3, (2016) 40, arXiv:1507.06424 [hep-ph].

[13] A. Pich, "The Standard model of electroweak interactions", in *High-energy physics. Proceedings, European School, Aronsborg, Sweden, June 18-July 1, 2006*, pp. 1–49. 2007. arXiv:0705.4264 [hep-ph]. http://doc.cern.ch/yellowrep/2007/2007-005/cern-2007-005.pdf.

[14] J. Gunion, R. Vega, and J. Wudka, "Higgs triplets in the standard model", *Physical Review D* 42 no. 5, (1990) 1673.

[15] P. Dey, A. Kundu, and B. Mukhopadhyaya, "Some consequences of a higgs triplet", *Journal of Physics G: Nuclear and Particle Physics* 36 no. 2, (2008) 025002.

[16] G. B. Gelmini and M. Roncadelli, "Left-Handed Neutrino Mass Scale and Spontaneously Broken Lepton Number", *Phys. Lett.* 99B (1981) 411–415.

[17] J. Bernabéu, A. Pich, and A. Santamaría, "CP phases in the charged current and Higgs sectors for Majorana neutrinos", *Zeitschrift für Physik C Particles and Fields* 30 no. 2, (1986) 213–220.

[18] C. Patrignani, P. Richardson, O. Zenin, R.-Y. Zhu, A. Vogt, S. Pagan Griso, L. Garren, D. Groom, M. Karliner, D. Asner, *et al.*, "Review of particle physics, 2016-2017", *Chin. Phys. C* 40 (2016) 100001.

[19] C. Bonilla, R. M. Fonseca, and J. W. Valle, "Consistency of the triplet seesaw model revisited", *Physical Review D* 92 no. 7, (2015) 075028.

[20] A. Arhrib, R. Benbrik, M. Chabab, G. Moultaka, M. Peyranere, L. Rahili, and J. Ramadan, "Higgs potential in the type ii seesaw model", *Physical Review D* 84 no. 9, (2011) 095005.

[21] D. Das and A. Santamaria, "Updated scalar sector constraints in the higgs triplet model", *Physical Review D* 94 no. 1, (2016) 015015.

[22] W. Konetschny and W. Kummer, "Nonconservation of total lepton number with scalar bosons", *Physics Letters B* 70 no. 4, (1977) 433–435.

[23] T. Cheng and L.-F. Li, "Neutrino masses, mixings, and oscillations in $SU(2)\times U(1)$ models of electroweak interactions", *Physical Review D* 22 no. 11, (1980) 2860.

[24] G. Lazarides, Q. Shafi, and C. Wetterich, "Proton lifetime and fermion masses in an SO(10) model", *Nuclear Physics B* 181 no. 2, (1981) 287–300.

[25] T. Blank and W. Hollik, "Precision observables in SU(2) x U(1) models with an additional Higgs triplet", *Nucl. Phys.* B514 (1998) 113–134, `arXiv:hep-ph/9703392 [hep-ph]`.

[26] Particle Data Group Collaboration, K. Nakamura *et al.*, "Review of particle physics", *J. Phys.* G37 (2010) 075021.

[27] J. F. Gunion, H. E. Haber, G. L. Kane, and S. Dawson, "The Higgs Hunter's Guide", *Front. Phys.* 80 (2000) 1–404.

[28] P. Fileviez Perez, T. Han, G.-y. Huang, T. Li, and K. Wang, "Neutrino Masses and the CERN LHC: Testing Type II Seesaw", *Phys. Rev.* D78 (2008) 015018, `arXiv:0805.3536 [hep-ph]`.

[29] A. Melfo, M. Nemevsek, F. Nesti, G. Senjanovic, and Y. Zhang, "Type II Seesaw at LHC: The Roadmap", *Phys. Rev.* D85 (2012) 055018, `arXiv:1108.4416 [hep-ph]`.

[30] CMS Collaboration, V. Khachatryan *et al.*, "Search for high-mass diphoton resonances in proton-proton collisions at 13 TeV and combination with 8 TeV search", *Phys. Lett.* B767 (2017) 147–170, `arXiv:1609.02507 [hep-ex]`.

[31] CMS Collaboration, A. M. Sirunyan *et al.*, "Search for high-mass $Z\gamma$ resonances in proton-proton collisions at $\sqrt{s} = 8$ and 13 TeV using jet substructure techniques", arXiv:1612.09516 [hep-ex].

[32] CMS Collaboration, V. Khachatryan *et al.*, "Search for Resonant Production of High-Mass Photon Pairs in Proton-Proton Collisions at $\sqrt{s}$ =8 and 13 TeV", *Phys. Rev. Lett.* 117 no. 5, (2016) 051802, arXiv:1606.04093 [hep-ex].

[33] CMS Collaboration, V. Khachatryan *et al.*, "Search for high-mass $Z\gamma$ resonances in $e^+e^-\gamma$ and $\mu^+\mu^-\gamma$ final states in proton-proton collisions at $\sqrt{s} = 8$ and 13 TeV", *JHEP* 01 (2017) 076, arXiv:1610.02960 [hep-ex].

[34] ATLAS Collaboration, T. A. collaboration, "Search for charged Higgs bosons in the $\tau+$ jets final state using 14.7 fb of pp collision data recorded at $\sqrt{s} = 13$ TeV with the ATLAS experiment",.

[35] ATLAS Collaboration, T. A. collaboration, "Search for charged Higgs bosons in the $H^{\pm} \to tb$ decay channel in pp collisions at $\sqrt{s} = 13$ TeV using the ATLAS detector",.

[36] CMS Collaboration, C. Collaboration, "Search for charged Higgs bosons with the $\mathrm{H}^{\pm} \to \tau^{\pm}\nu_{\tau}$ decay channel in the fully hadronic final state at $\sqrt{s} = 13$ TeV",.

[37] CMS Collaboration, A. M. Sirunyan *et al.*, "Search for charged Higgs bosons produced in vector boson fusion processes and decaying into a pair of W and Z bosons using proton-proton collisions at sqrt(s) = 13 TeV", arXiv:1705.02942 [hep-ex].

[38] E. Asakawa and S. Kanemura, "The $H^{\pm}W^{\mp}Z^0$ vertex and single charged Higgs boson production via WZ fusion at the Large Hadron Collider", *Physics Letters B* 626 no. 1, (2005) 111 – 119. http://www.sciencedirect.com/science/article/pii/S0370269305011482.

[39] J. F. Gunion, R. Vega, and J. Wudka, "Higgs triplets in the standard model", *Phys. Rev. D* 42 (Sep, 1990) 1673–1691. https://link.aps.org/doi/10.1103/PhysRevD.42.1673.

[40] CMS Collaboration, C. Collaboration, "A search for doubly-charged Higgs boson production in three and four lepton final states at $\sqrt{s} = 13$ TeV",.

[41] E. S. Abers and B. W. Lee, "Gauge theories", *Physics Reports* 9 no. 1, (1973) 1–2.

[42] T.-P. Cheng, L.-F. Li, and T.-P. Cheng, "Gauge theory of elementary particle physics",.